

Текущее состояние и физические задачи эксперимента MPD на коллайдере NICA

В.Г. Рябов



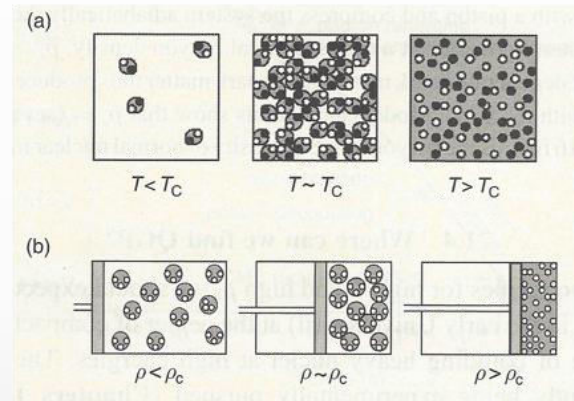
Heavy-ion collisions

- ❖ QCD is a fundamental theory of strong interactions
- ❖ Only colorless particles observed in the experiment (no free quarks or gluons) → confinement
- ❖ QGP is a state of matter in which quarks and gluons are free to move in space \gg size of the nucleon
- ❖ QGP matter formation:

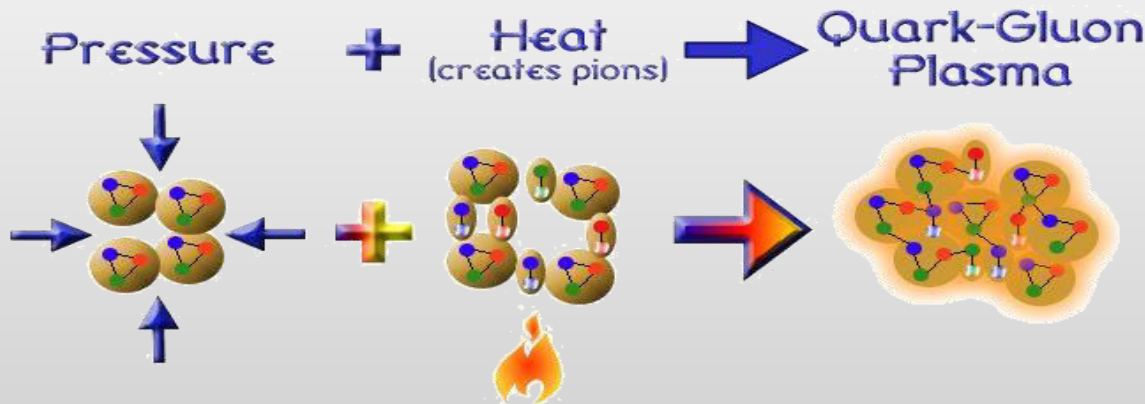
Two recipes:

(a) at high T - Early universe

(b) at high baryon density – Neutron stars

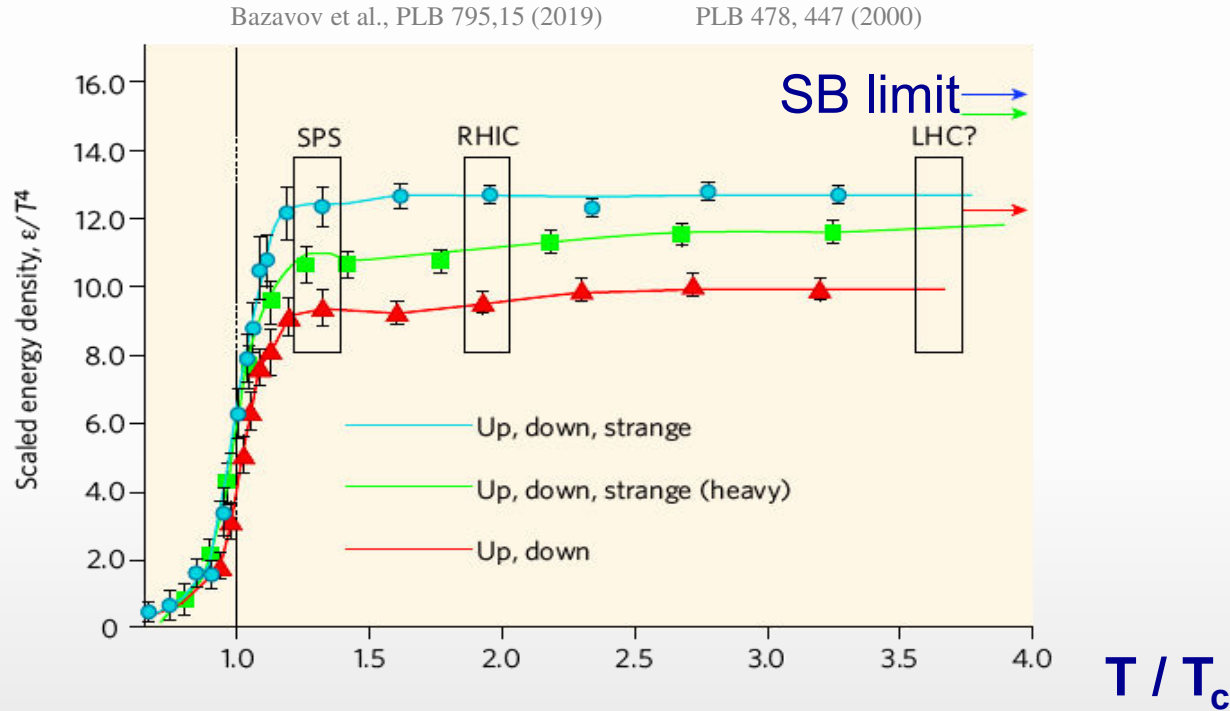


Relativistic heavy ion collisions - A combination of the two recipes



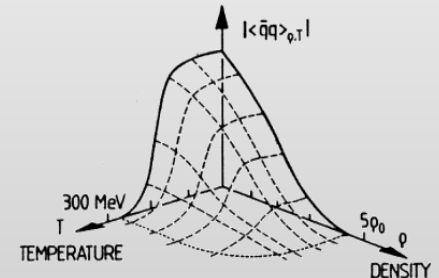
LQCD calculations

- ❖ The QGP is predicted by numerical calculations of QCD on the lattice

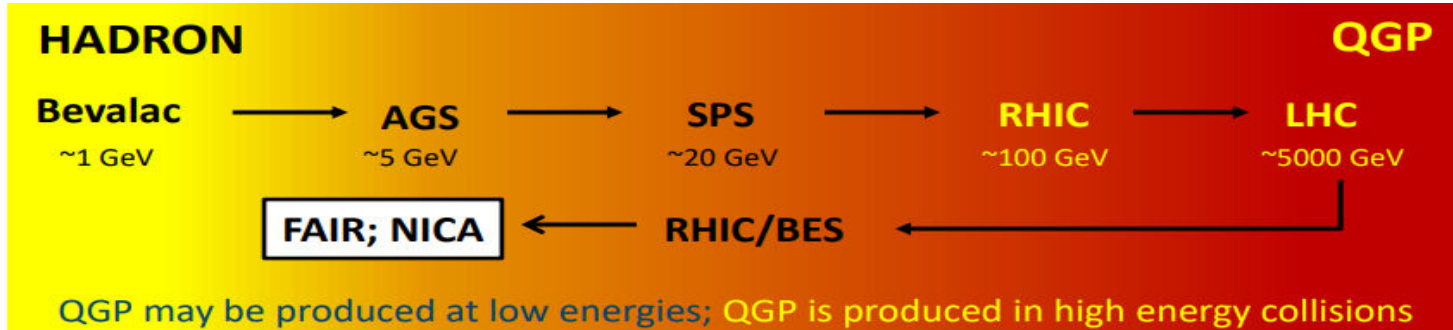


Recent LQCD calculations show that the critical temperature is: T_c (at $\mu_B = 0$) = 156.5 ± 1.5 MeV

- ❖ Accompanied by chiral symmetry restoration → constituent quark mass ~ 300 MeV turns into current quark mass $\sim 5-10$ MeV



Heavy-ion collisions

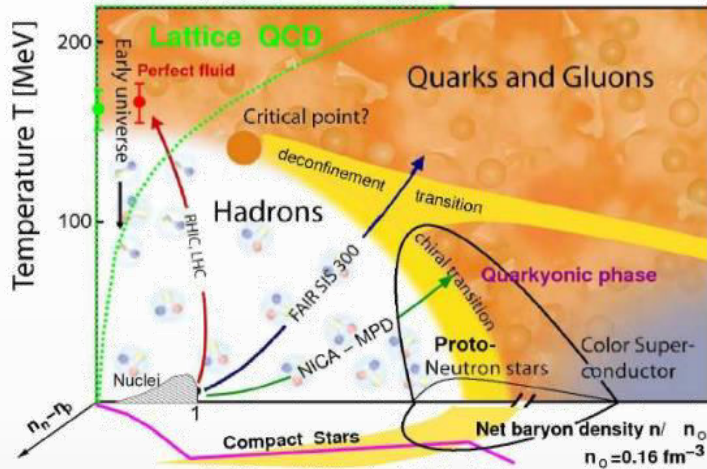


Short heavy-ion physics history

- | | | | |
|---|--------------------------------|--|-------------------------|
| ❖ BEVALAC – LBNL 1972-1984 | max. $\sqrt{s_{NN}} = 2.2$ GeV | | Fixed target |
| ❖ SPS – CERN 1986-2000 | $\sqrt{s_{NN}} = 17.3$ GeV | NA35/49, NA44, NA38/50/51, NA45, NA52, NA57, NA60, WA80/98, WA97 ... | |
| ❖ AGS – BNL 1988-1996 | $\sqrt{s_{NN}} = 4.8$ GeV | E864/941, E802/859/866/917, E814/877, E858/878, E810/891, E896, E910 ... | |
| ❖ SIS18 – GSI 1990 \rightarrow | $\sqrt{s_{NN}} = 2.4$ GeV | | |
| ❖ RHIC – BNL 2000-2025 | $\sqrt{s_{NN}} = 200$ GeV | BRAHMS, PHENIX, PHOBOS, STAR | Collider |
| ❖ LHC – CERN 2010 \rightarrow | $\sqrt{s_{NN}} = 5.02$ TeV | ALICE, ATLAS, CMS, LHCb | |
| Near future | | | |
| ❖ NICA – JINR 2024 | $\sqrt{s_{NN}} = 11$ GeV | MPD, BM@N | Collider & Fixed target |
| ❖ SIS100 – FAIR 2028? | $\sqrt{s_{NN}} = 5$ GeV | CBM, HADES | Fixed target |

Heavy-ion collisions

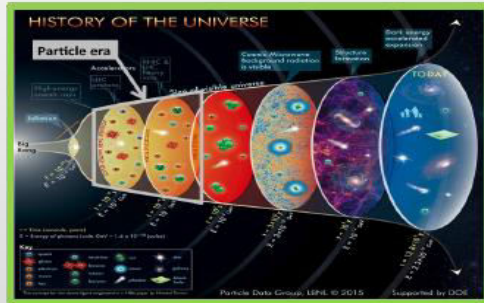
- ❖ Study QCD under extreme conditions of temperature and density
- ❖ Explore the QCD phase diagram, search for the QGP and study its properties



Why Quark-gluon plasma is of interest?

- ✓ primordial form of QCD matter at high temperatures and/or (net)baryon densities
- ✓ present during the first microseconds after Big Bang and in cores of the compact neutron stars / mergers
- ✓ provides important insights on the origin of mass for matter, and how quarks are confined into hadrons

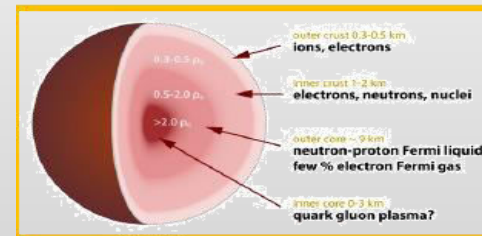
High beam energies ($\sqrt{s_{NN}} > 100$ GeV)



High temperature:
Early Universe evolution

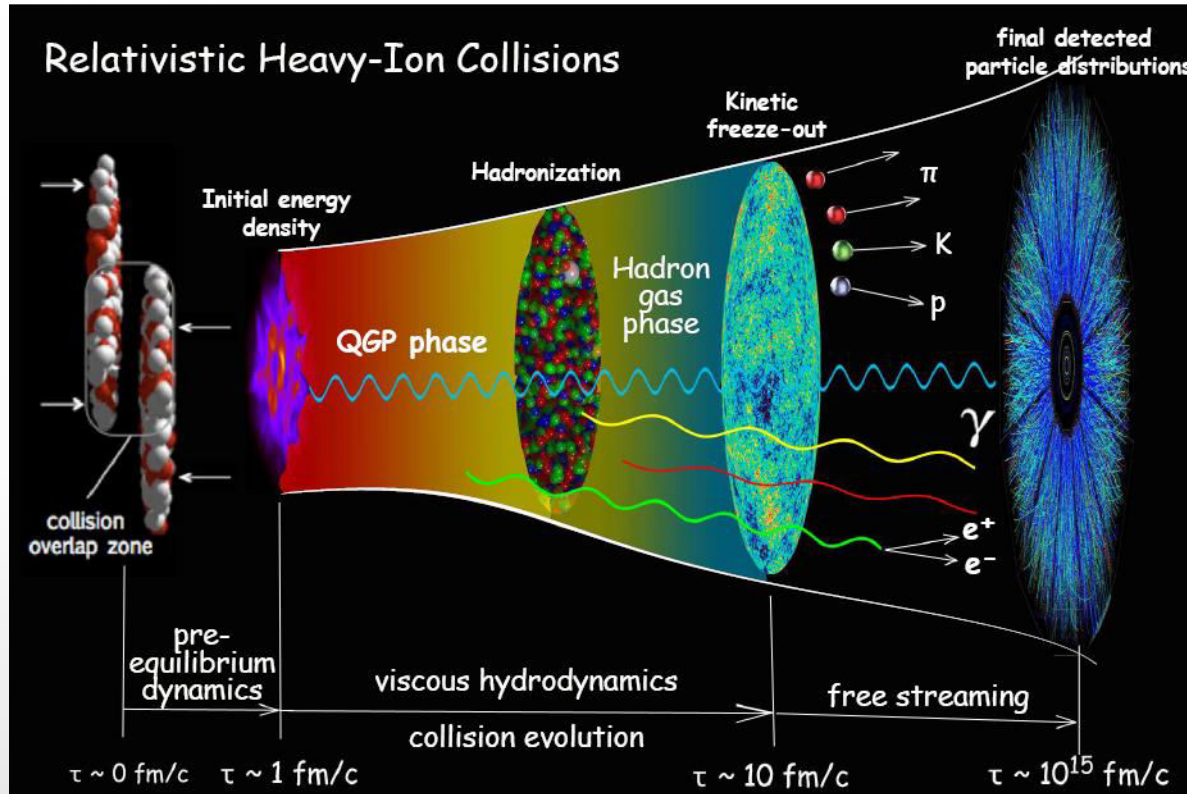
Low beam energies ($\sqrt{s_{NN}} \sim 10$ GeV)

High baryon density:
Inner structure of
compact stars

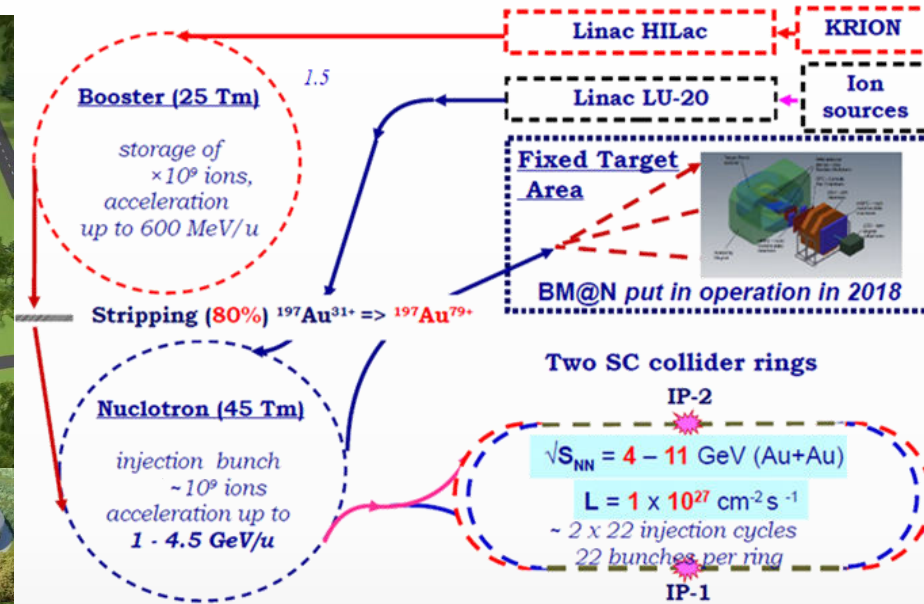
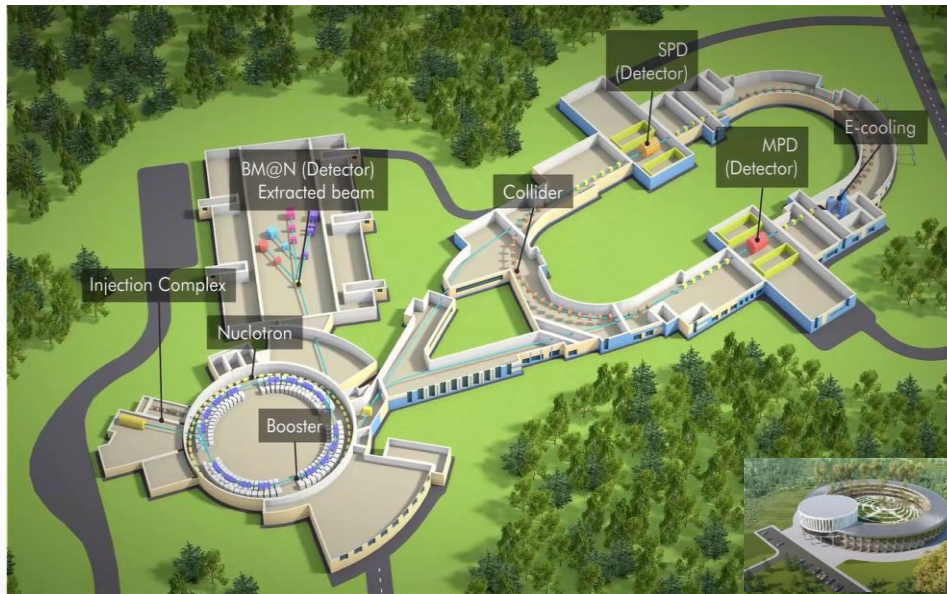


System evolution in heavy-ion collisions

Fireball is $\sim 10^{-15}$ meters across and lives for 5×10^{-23} seconds

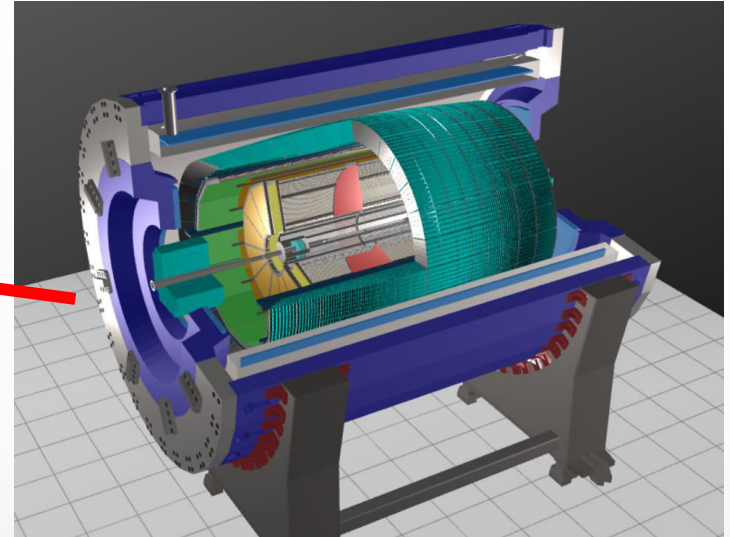
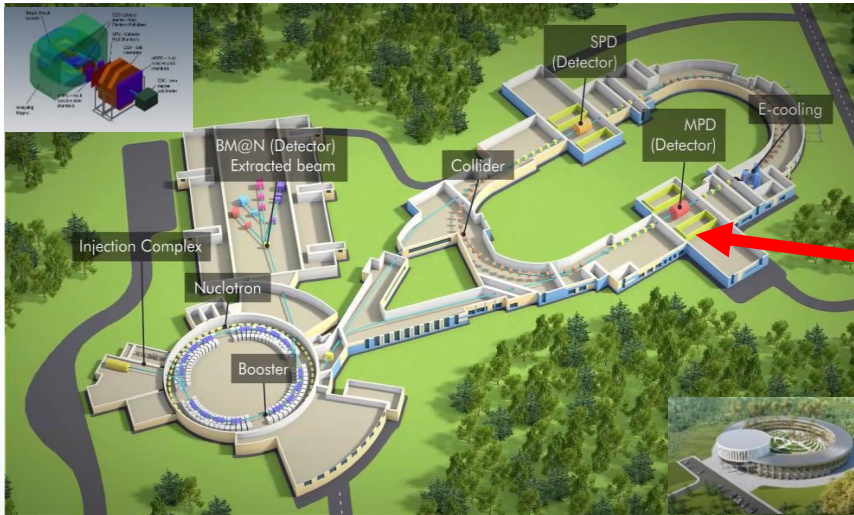


- ❖ Only final state particles are measured in the detector: γ , e^\pm , μ^\pm , π^0 , π^\pm , K^0 , K^\pm , η , ω , p , \bar{p} , ϕ , Λ , Σ , Ξ , etc.
- ❖ The measurements are used to infer properties of the early state of relativistic heavy-ion collisions by comparing measurement results with model (post)predictions



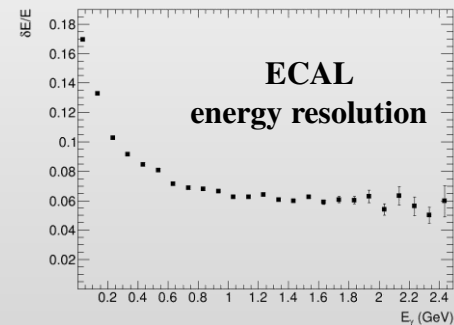
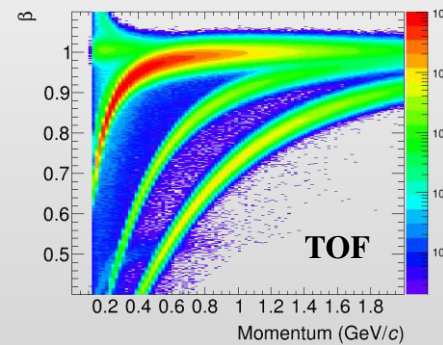
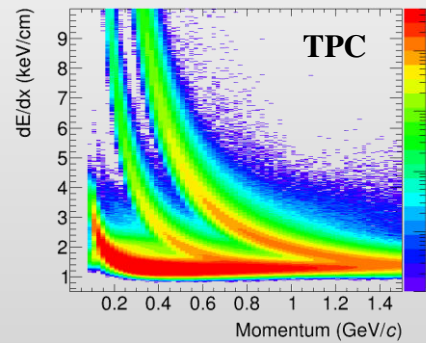
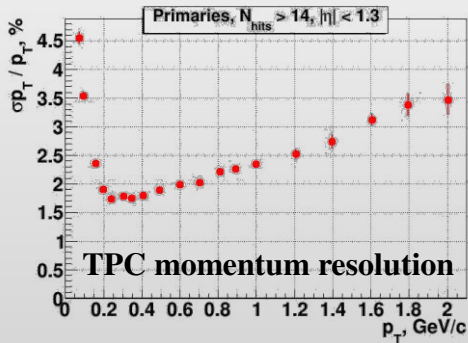
- ❖ The first megascience project in Russia, which is approaching its full commissioning:
 - ✓ already running in the fixed-target mode – BM@N
 - ✓ start of operation in collider mode in 2025 – MPD and later SPD

❖ One of two experiments at NICA collider to study heavy-ion collisions at $\sqrt{s_{NN}} = 4-11$ GeV

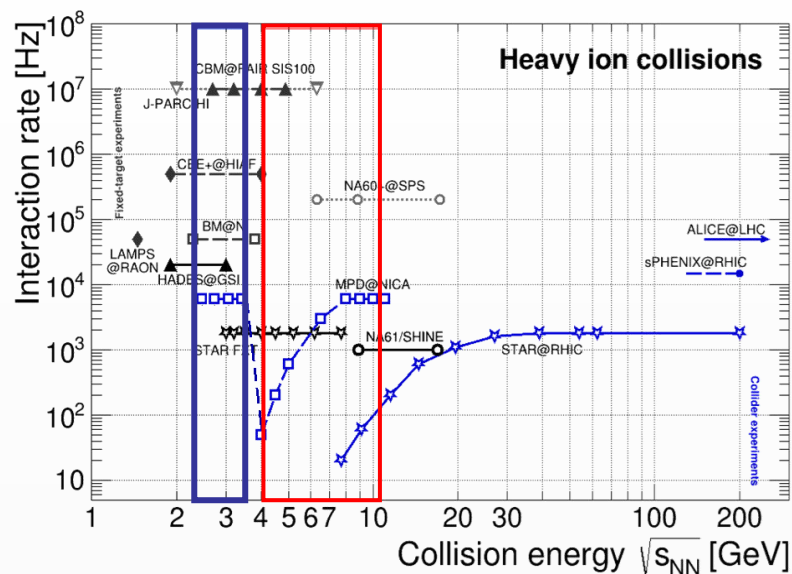
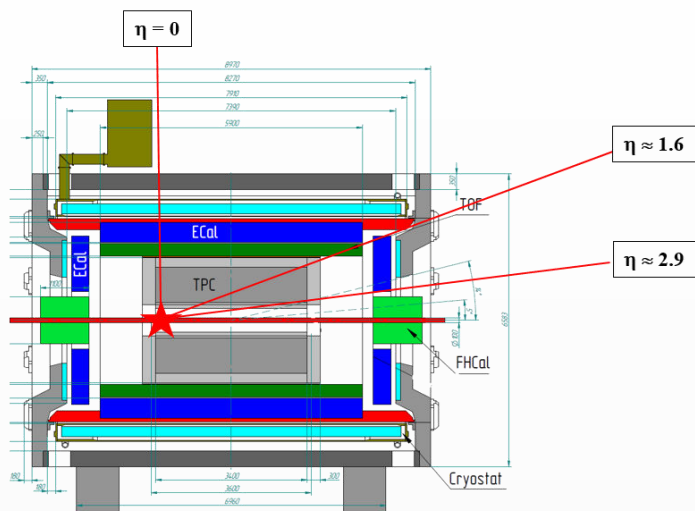


TPC: $|\Delta\phi| < 2\pi$, $|\eta| \leq 1.6$; TOF, EMC: $|\Delta\phi| < 2\pi$, $|\eta| \leq 1.4$; FFD: $|\Delta\phi| < 2\pi$, $2.9 < |\eta| < 3.3$; FHCAL: $|\Delta\phi| < 2\pi$, $2 < |\eta| < 5$

Au+Au @ 11 GeV (UrQMD + full chain reconstruction)



Fixed-target operation



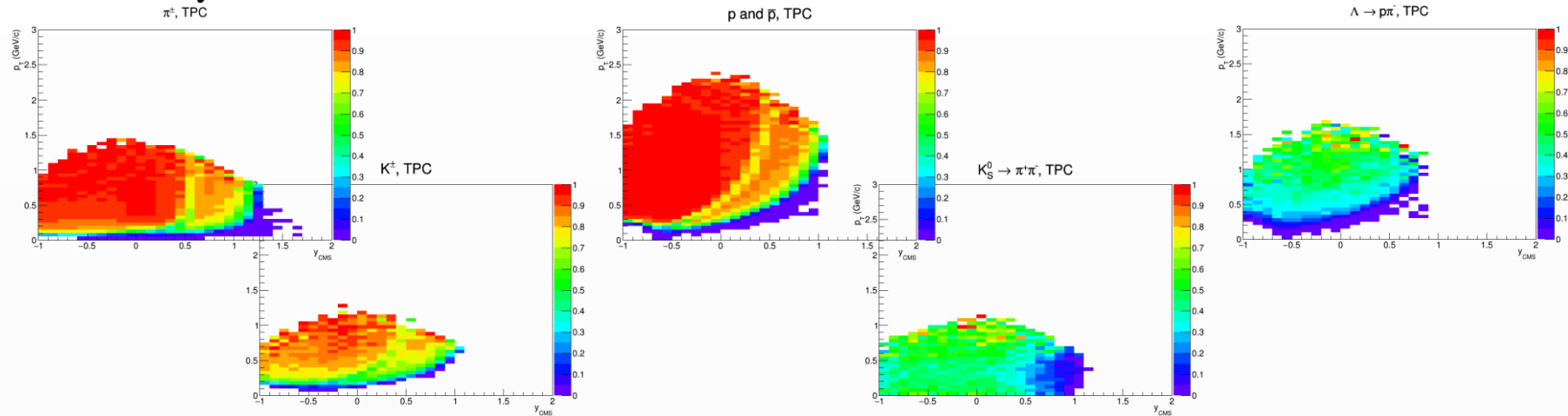
- ❖ MPD-CLD and MPD-FXT options approved by accelerator department (now a default option)
- ❖ Collider mode, $\sqrt{s_{NN}} = 4$ -11 GeV
- ❖ Fixed-target mode: one beam + thin wire ($\sim 100 \mu\text{m}$) close to the edge of the MPD central barrel:
 - ✓ extends energy range of MPD to $\sqrt{s_{NN}} = 2.4$ -3.5 GeV (overlap with HADES, BM@N and CBM)
 - ✓ solves problem of low event rate at lower collision energies (only ~ 50 Hz at $\sqrt{s_{NN}} = 4$ GeV at design luminosity)
- ❖ Expected beam condition for the first year(s):
 - ✓ MPD-CLD: Xe+Xe at $\sqrt{s_{NN}} \leq 7$ GeV, reduced luminosity \rightarrow collision rate ~ 50 Hz
 - ✓ MPD-FXT: Xe+W at $\sqrt{s_{NN}} \leq 2.8$ GeV

Capability of target and collision energy overlap between MPD and BM@N experiments

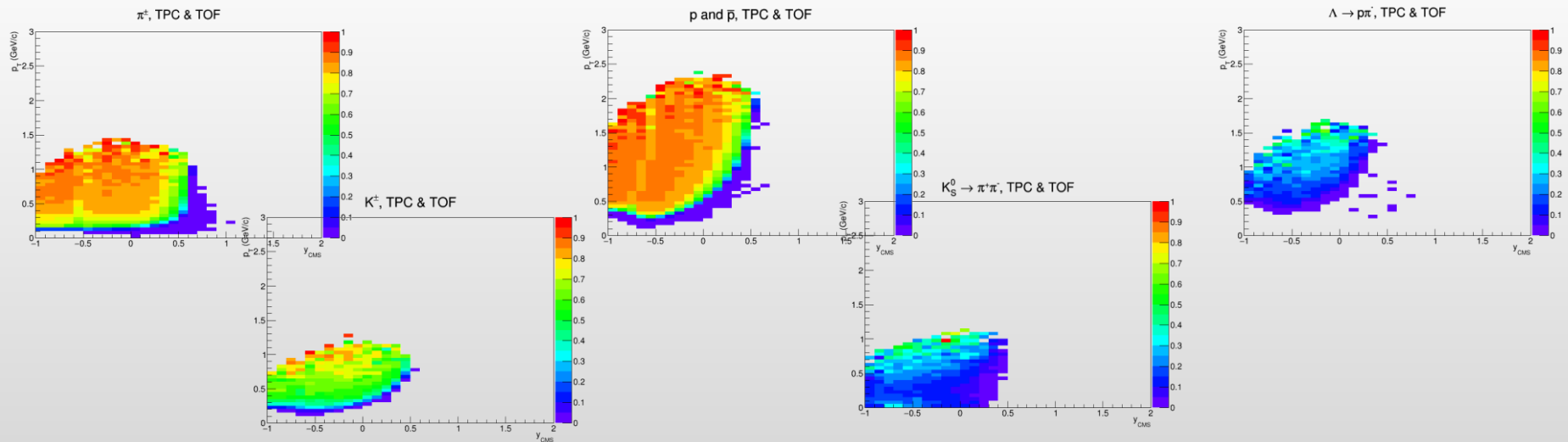
Efficiency for $\pi/K/p/Ks/\Lambda$, $z_{\text{vertex}} = -85$ cm

Basic track selections: $N_{\text{hits}} > 10$; $DCA < 2$ cm; Primary particles ($R_{\text{production}} < 1$ cm)

❖ TPC-only tracks:



❖ TPC + TOF tracks:

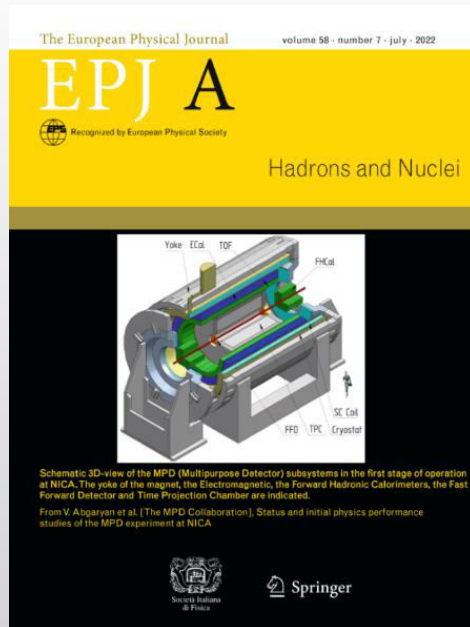


Reasonable coverage at mid-rapidity for light and heavy identified hadrons

- ❖ MPD strategy – high-luminosity scans in **energy** and **system size** to measure a wide variety of signals:
 - ✓ order of the phase transition and search for the QCD critical point → structure of the QCD phase diagram
 - ✓ hypernuclei and equation of state at high baryon densities → inner structure of compact stars, star mergers
- ❖ Scans to be carried out using the **same apparatus** with all the advantages of collider experiments:
 - ✓ maximum phase space, minimally biased acceptance, free of target parasitic effects
 - ✓ correlated systematic effects for different systems and energies → simplified extraction of physical signals
- ❖ Continuously develop physical program based on the recent advancements in the field:

First collaboration paper recently published EPJA (~ 50 pages): Eur.Phys.J.A 58 (2022) 7, 140

Status and initial physics performance studies of the MPD experiment at NICA



Eur. Phys. J. A manuscript No.
(will be inserted by the editor)

Status and initial physics performance studies of the MPD experiment at NICA

The MPD Collaboration¹
¹The full list of Collaboration Members is provided at the end of the manuscript

Received: April 20, 2022 / Accepted: date

Abstract The **Nucleon-based Ion Collider Facility (NICA)** is under construction at the **Joint Institute for Nuclear Research (JINR)**, with commissioning of the facility expected in late 2022. The **Multi-Purpose Detector (MPD)** has been designed to operate at NICA, and its components are currently in production. The detector is expected to be ready for data taking with the first beams from NICA. This document provides an overview of the landscape of the investigation of the QCD phase diagram in the region of maximum baryon density, where NICA and MPD will be able to provide significant and unique input. It also provides a detailed description of the MPD set-up, including its various subsystems as well as its support and computing infrastructure. Selected performance studies for particle and physics measurements at MPD are presented and discussed in the context of existing data and theoretical expectations.

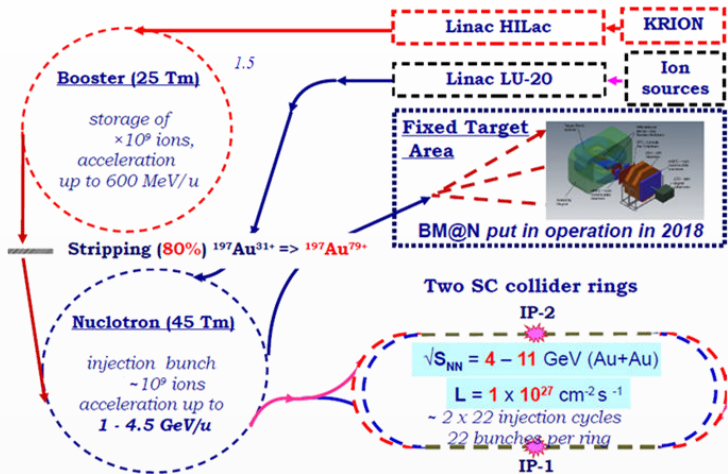
Keywords NICA · MPD · QCD

Contents

1. Introduction	1
2. The Multi-Purpose Detector (MPD) physics goals	4
3. The detector components	7
4. The magnet	7
5. The electromagnetic calorimeters	10
6. The forward hadronic calorimeters	10
7. The fast forward detector	12
8. The time projection chamber	12
9. The particle identification system	15
10. The particle tracking system	15
11. The particle identification system	15
12. The particle identification system	15
13. The particle identification system	15
14. The particle identification system	15
15. The particle identification system	15
16. The particle identification system	15
17. The particle identification system	15
18. The particle identification system	15
19. The particle identification system	15
20. The particle identification system	15
21. The particle identification system	15
22. The particle identification system	15
23. The particle identification system	15
24. The particle identification system	15
25. The particle identification system	15
26. The particle identification system	15
27. The particle identification system	15
28. The particle identification system	15
29. The particle identification system	15
30. The particle identification system	15
31. The particle identification system	15
32. The particle identification system	15
33. The particle identification system	15
34. The particle identification system	15
35. The particle identification system	15
36. The particle identification system	15
37. The particle identification system	15
38. The particle identification system	15
39. The particle identification system	15
40. The particle identification system	15
41. The particle identification system	15
42. The particle identification system	15
43. The particle identification system	15
44. The particle identification system	15
45. The particle identification system	15
46. The particle identification system	15
47. The particle identification system	15
48. The particle identification system	15
49. The particle identification system	15
50. The particle identification system	15

1 Introduction

The Multi-Purpose Detector (MPD) is one of the new dedicated heavy-ion collision experiments of the Nucleon-based Ion Collider Facility (NICA), one of the flagship projects, planned to come into operation at the Joint Institute for Nuclear Research (JINR) in 2022. Its main scientific purpose is to search for novel phenomena in the baryon-rich region of the QCD phase diagram by means of colliding heavy nuclei in the energy range of $1 \text{ GeV} < \sqrt{s_{NN}} < 11 \text{ GeV}$.



Booster



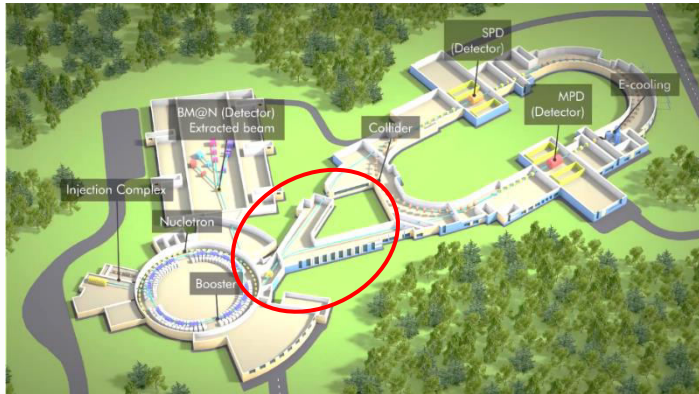
Nuclotron



❖ Stages of the accelerator complex commissioning

- ✓ HILAC + transfer line to Booster → commissioned in 2018 with He^{1+} , Fe^{14+} , C^{4+} , Ar^{14+} and Xe^{28+}
- ✓ HILAC + Booster → first run in November-December, 2020 with He^{1+}
- ✓ HILAC + Booster + transfer line to Nuclotron → second run in October, 2021 with He^{1+} and Fe^{16+}
- ✓ HILAC + Booster + Nuclotron + transfer line to BM@N → third run in Jan. – Apr., 2022 with C^{6+}
- ✓ HILAC + Booster + Nuclotron + transfer line to BM@N → fourth run in September, 2022 – February, 2023 with Ar and Xe beams → 500+ M events at BM@N

Nuclotron-NICA transfer line

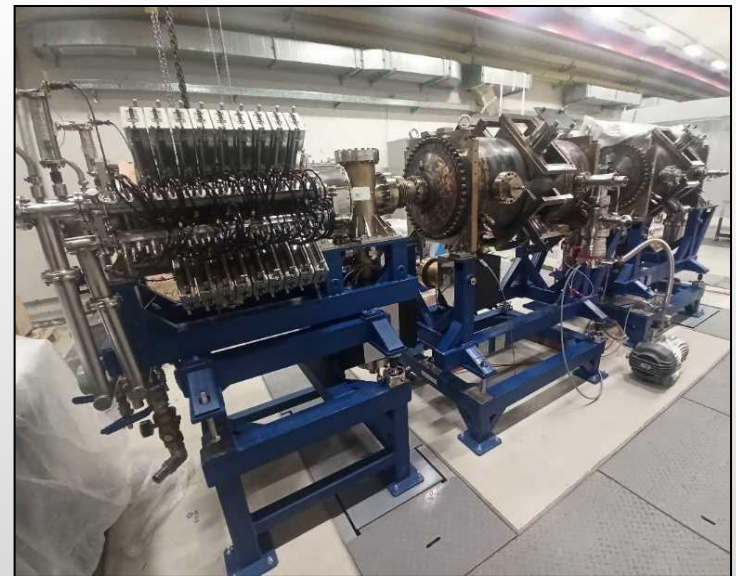


NICA collider

заканчивается установка диполей и квадруполей в туннеле



ВЧ-1 и четыре ВЧ-2 (ИЯФ СО РАН) установлены в туннеле



- ❖ Magnet and RF installation – nearly finalized
- ❖ First technological and cryogenic run of collider: end of 2024 - beginning of 2025
- ❖ Fast extraction system from the Nuclotron: middle of 2024
- ❖ Nuclotron-collider transfer line: Autumn of 2024
- ❖ First run with beams: 2025

Cryogenic platform



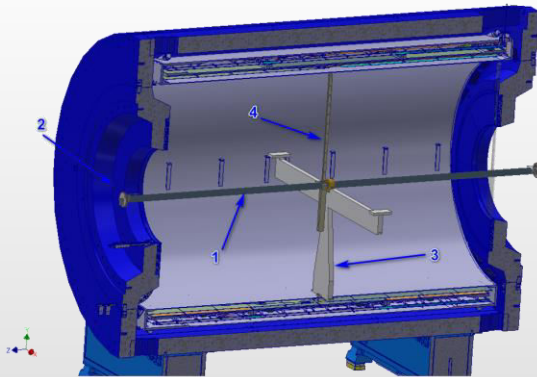
Chimney



Cryogenic pipes



Novosibirsk BINP magnetic field mapper



1. Aluminum (carbon fiber plastic) guiding rod
2. End cap fixation
3. Intermediate support
4. Carbon fiber plastic carriage

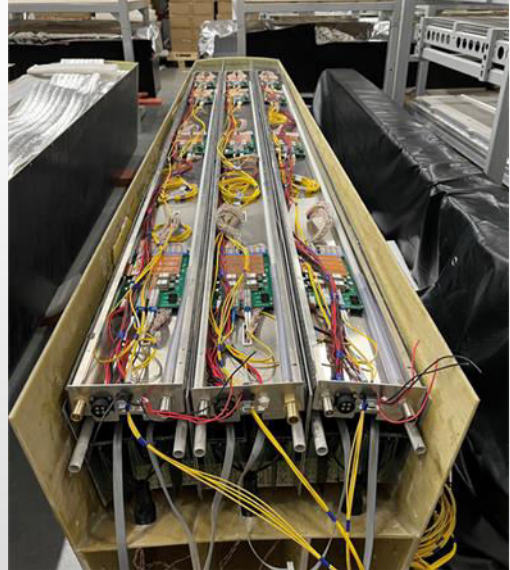
Parameter	Value
Length of movement for Z	2 × 4.5 m
Length of movement for R	0.1 – 2.2 m
Rotation of measurement block	3600
Accuracy of movement for Z	50 microns
Accuracy of movement for R	50 microns
Accuracy of rotation	0.20
Hall 3D sensor	HE444, HE Hoeben Electronix,
Hall 3D sensor accuracy	0.1 Gs
Hall 3D sensor accuracy total (with accuracy of laser tracker and temperature correction)	0.3 Gs
Sag of guide line	5 mm
Weight of mapper	100 kg
Reading time per one measurement	1 sec

Carbon fiber support frame sagita ~ 5 mm at full load



- ❖ Test cooling to 70⁰ K in February-March
- ❖ Cooling to LHe → second half of 2024 → MF measurements → installation of carbon fiber support frame and subsystems

- ❖ Sampling calorimeter with projective geometry (70 tons): 38,400 towers packed in 50 half-sectors
- ❖ First 1600 modules (66%, 800 in Russia + 800 in China): tested/calibrated and mounted into half-sectors
- ❖ Installation of electronics and cooling system in assembled half-sectors → to be finished by March, 2024
- ❖ Long-term stability test of ECAL half-sectors using LED monitoring system
- ❖ Finalizing production of additional 400 modules (+12.5% → 83% in total)
- ❖ Production of components (including WLS) for the remaining 400 modules (+12.5% → 100% in total)
- ❖ Electronics: produced, in stock



- ❖ Production of MRPC detectors was completed in September 2022, (107%) chambers
- ❖ All 28 TOF modules are assembled → long-term cosmic ray tests
- ❖ Electronics & cables, HV distribution modules → in stock
- ❖ Assembled the TOF gas system in the MPD hall

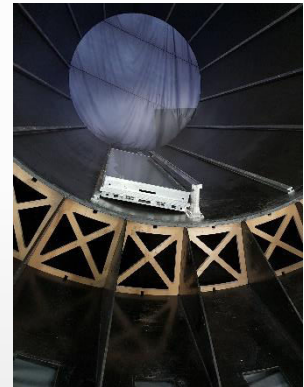
Storage of tested TOF modules



TOF installation bench in LHEP



TOF module in the carbon fiber mainframe



- ❖ Equipment for installing the modules in the MPD is ready for use and stored in the laboratory

- ❖ TPC cylinders, central membrane and service wheels are ready
- ❖ Assembly of the vessel with field cage is ongoing – full TPC assembly by November, 2024
- ❖ Read-out MWPC chambers (ROCs) – 28 out of 24 (12x2) needed are produced and tested



- ❖ LV/HV: CAEN based, purchased
- ❖ FEC (1488 pcs.): 100% components are available
- ❖ RCU (24 pcs.): 1st version tested, finalizing design of preproduction version
- ❖ DCU (6 pcs.), LDC (6 pcs.): based on commercial solutions - available
- ❖ Gas system: ready, testing
- ❖ DCS: in development
- ❖ TPC cooling: thermostabilization panels and FEE radiators in stock; TPC cooling system – (INP BSU, Belarus) assembled by September, 2024

FHCAL

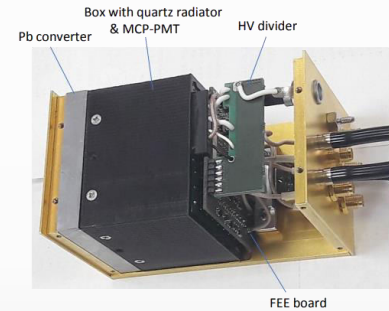
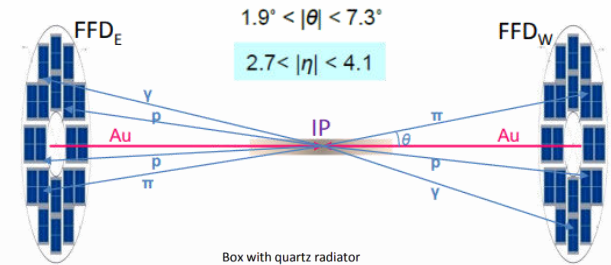


FHCAL assembled on the platform is ready to be installed in the Pole.



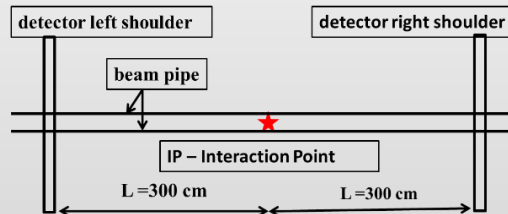
FHCAL modules have been produced and tested → installation in autumn 2023

FFD



Cherenkov modules of FFDE and FFDW are available, mechanics of FFD sub-detectors is available for installation in container with vacuum beam tube

Beam and luminosity monitoring



Measurement of transverse sizes of the bunches
 Transvers and longitudinal convergence of bunches
 Vertices distribution along the beam

- ❖ Two sets by 32 scintillator counters readout by SIMPs from both sides
- ❖ Observables & methods:
 - ✓ counting rate and z-vertex distribution ($\sigma_{z\text{-vertex}} \sim 5 \text{ cm}$ with $\delta\tau \sim 300 \text{ ps}$)
 - ✓ Van der Meer and ΔZ scans for optimization of beam optics
- ❖ Beam tests of prototypes
- ❖ Mass production of scintillator detectors

G. Feofilov, P. Parfenov

Global observables

- Total event multiplicity
- Total event energy
- Centrality determination
- Total cross-section measurement
- Event plane measurement at all rapidities
- Spectator measurement

V. Kolesnikov, Xianglei Zhu

Spectra of light flavor and hypernuclei

- Light flavor spectra
- Hyperons and hypernuclei
- Total particle yields and yield ratios
- Kinematic and chemical properties of the event
- Mapping QCD Phase Diag.

K. Mikhailov, A. Taranenko

Correlations and Fluctuations

- Collective flow for hadrons
- Vorticity, Λ polarization
- E-by-E fluctuation of multiplicity, momentum and conserved quantities
- Femtoscopy
- Forward-Backward corr.
- Jet-like correlations

D. Peresunko, Chi Yang

Electromagnetic probes

- Electromagnetic calorimeter meas.
- Photons in ECAL and central barrel
- Low mass dilepton spectra in-medium modification of resonances and intermediate mass region

Wangmei Zha, A. Zinchenko

Heavy flavor

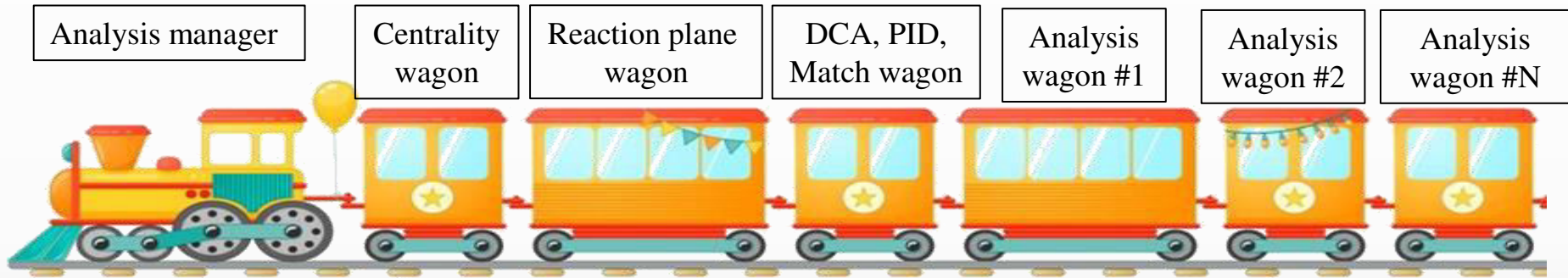
- Study of open charm production
- Charmonium with ECAL and central barrel
- Charmed meson through secondary vertices in ITS and HF electrons
- Explore production at charm threshold

- ❖ Physics feasibility studies using centralized large-scale MC productions → consistent picture of the MPD physics capabilities with the first data sets, preparation for real data analyses
- ❖ <https://mpdforum.jinr.ru/c/mcprod/26>:
 - Request 25: General-purpose, 50M UrQMD BiBi@9.2 → **DONE**
 - Request 26: General-purpose (trigger), 1M DCM-QGSM-SMM BiBi@9.2 → **DONE**
 - Request 27: General-purpose (trigger), 1M PHQMD BiBi@9.2 → **DONE**
 - Request 28: General-purpose with reduced magnetic field, 10M UrQMD BiBi@9.2 → **DONE**
 - Request 29: General-purpose (hypernuclei), 20M PHQMD BiBi@9.2 → **DONE**
 - Request 30: General-purpose (polarization), 15M PHSD BiBi@9.2 → **DONE**
 - Request 31: General-purpose (femtoscapy), 50 M UrQMD BiBi@9.2 with freeze-out → **DONE**
 - Request 32: General purpose (flow), 15M vHLLE+UrQMD with XPT → **DONE**
 - Request 33: General purpose (FXT), (11M x 3 energies) UrQMD (mean field) → **DONE**
- ❖ Production comparable in size to the first expected real data samples test the existing computing and software infrastructure
- ❖ Develop realistic analysis methods and techniques, set priorities and find group leaders

Handling the big data sets

- ❖ Centralized Analysis Framework for access and analysis of data → Analysis Train:
 - ✓ consistent approaches and results across collaboration, easier storage and sharing of codes and methods
 - ✓ reduced number of input/output operations for disks and databases, easier data storage on tapes

- ❖ Analysis manager reads event into memory and calls wagons one-by-one to modify and/or analyze data:



- ❖ The Analysis manager and the first Wagons have been created, in MpdRoot @ mpdroot/physics
- ❖ Eventually all analysis codes will be committed to MpdRoot as Wagons
- ❖ First Analysis Train runs started in September, 2023 → regular runs on request ever since
- ❖ 50M events are processed in ~ 10 hours with ~ 15 wagons (1 year of CPU time)

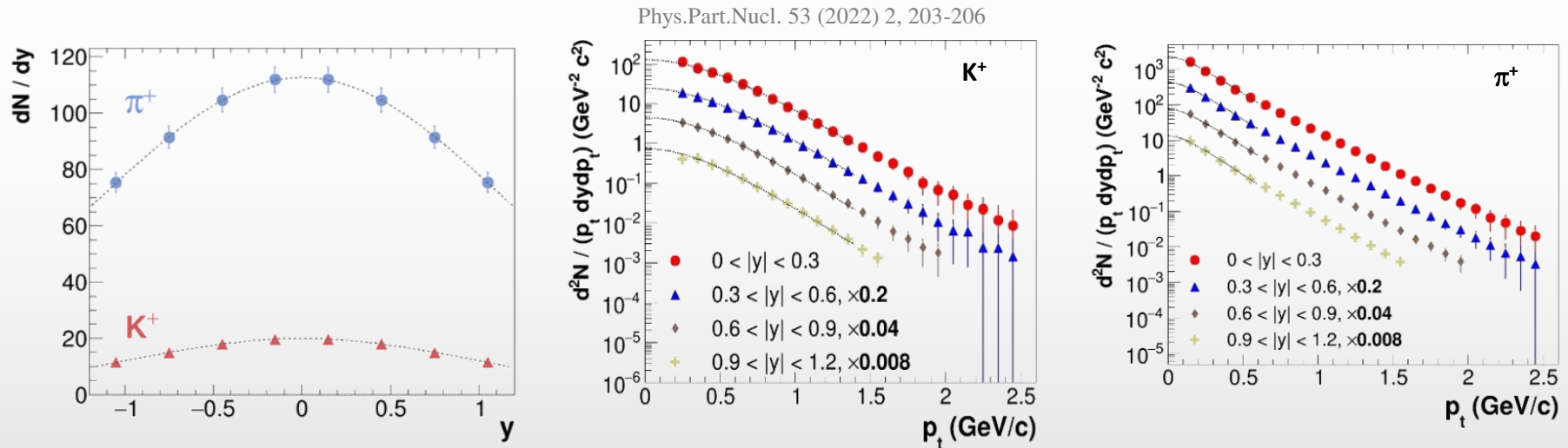
initial state

QGP as a
relativistic
fluid

Identified hadrons

- ❖ Probe freeze-out conditions, collective expansion, hadronization mechanisms, strangeness production (“horn” for K/π), parton energy loss, etc. with particles of different masses, quark contents/counts
- ❖ Charged hadrons: large and uniform acceptance + excellent PID capabilities of TPC and TOF

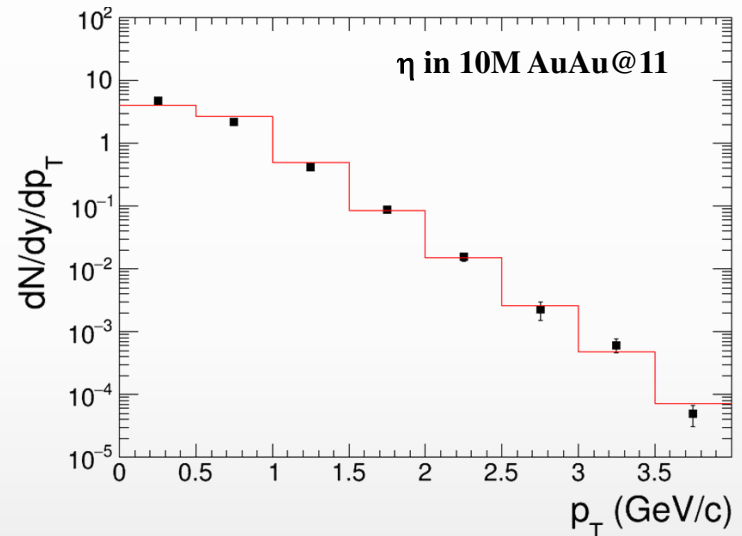
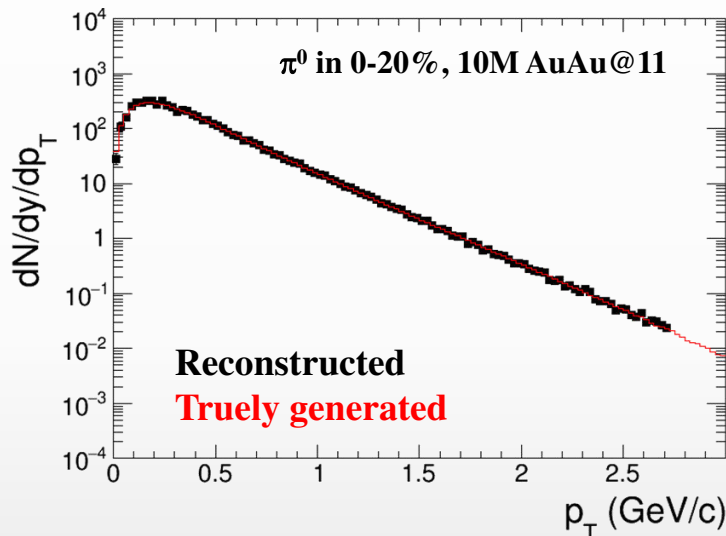
0-5% central AuAu@9 GeV (PHSD), 5 M events \rightarrow full event/detector simulation and reconstruction



- ✓ sample $\sim 70\%$ of the $\pi/K/p$ production in the full phase space
- ✓ hadron spectra are measured from $p_T \sim 0.1$ GeV/c

- ❖ Neutral mesons (π^0 , η , K_s , ω , η'): ECAL reconstruction + photon conversion method (PCM)
 π^0 ($\pi^0 \rightarrow \gamma\gamma$); η ($\eta \rightarrow \gamma\gamma$, $\eta \rightarrow \pi^0 \pi^+ \pi^-$); K_s ($K_s \rightarrow \pi^0 \pi^0$); ω ($\omega \rightarrow \pi^0 \gamma$, $\omega \rightarrow \pi^0 \pi^+ \pi^-$); η' ($\eta' \rightarrow \eta \pi^+ \pi^-$); etc.

AuAu@11 GeV (UrQMD), 10M events \rightarrow full event/detector simulation and reconstruction



- ✓ extend p_T ranges of charged particle measurements
- ✓ different systematics

MPD will be able to measure differential production spectra, integrated yields and $\langle p_T \rangle$, particle ratios, multiplicity distributions for a wide variety of identified hadrons (π , K , η , ω , p , η')

First measurements will be possible with the first sampled data sets

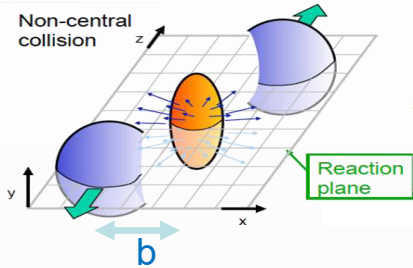
initial state

QGP as a
relativistic
fluid

Collective flow

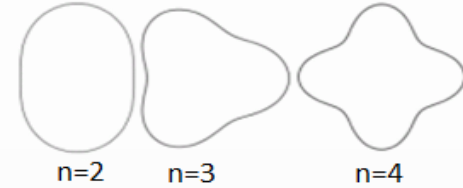
- ❖ Initial eccentricity and its fluctuations drive momentum anisotropy v_n with specific viscous modulation

Spatial anisotropy of the nuclear overlap region



$$\epsilon_n = \sqrt{\frac{\langle r^n \cos n\phi \rangle + \langle r^n \sin n\phi \rangle}{\langle r^n \rangle}}$$

Azimuthal distribution of produced particles wrt to reaction plane (Ψ_n)



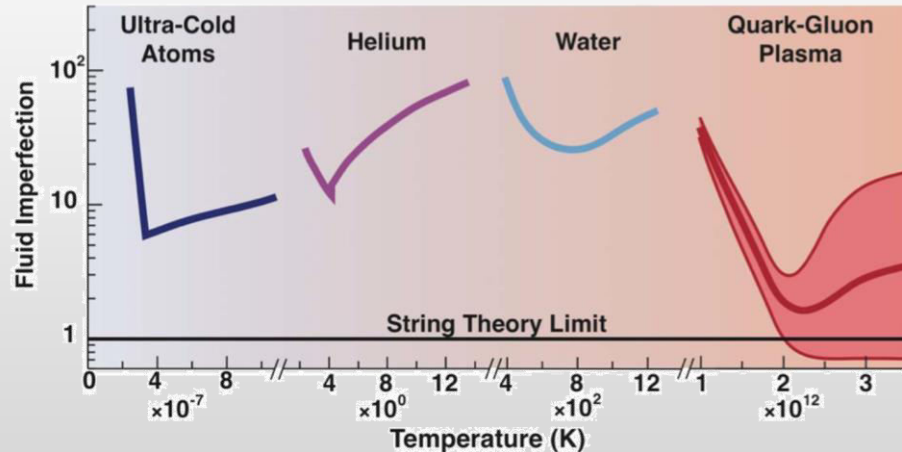
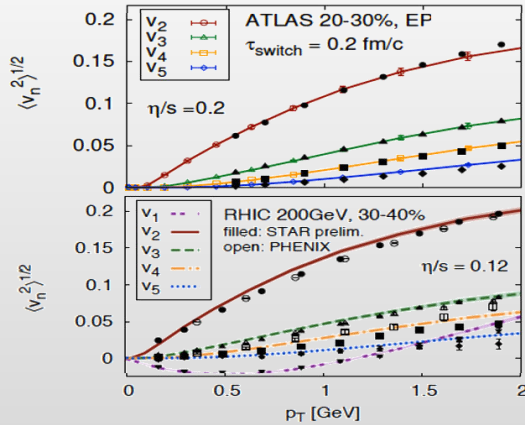
$$\epsilon_n \propto v_n$$

$$\frac{dN}{d\phi} \propto \left(1 + 2 \sum_{n=1} v_n \cos[n(\phi - \Psi_n)] \right)$$

Anisotropic flow: $v_n = \langle \cos[n(\phi - \Psi_n)] \rangle$

- ❖ Evidence for a dense perfect liquid found at RHIC/LHC

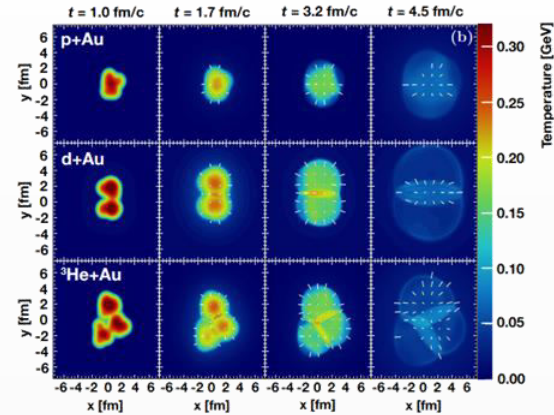
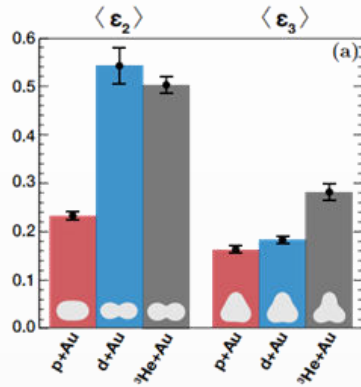
Gale, Jeon et al., Phys. Rev. Lett. 110, 012302



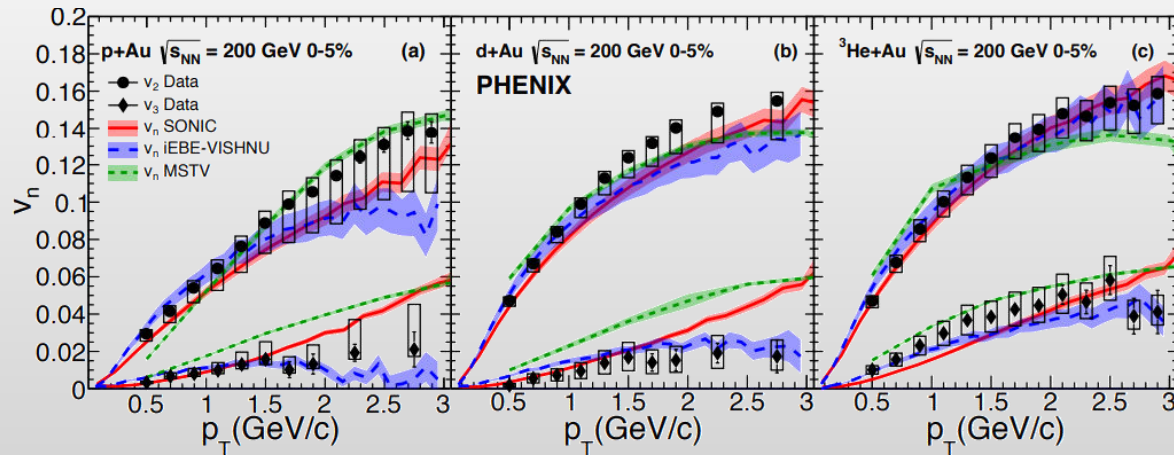
- ❖ System size scan (A-A): initial geometry \rightarrow flow harmonics $\rightarrow \frac{\eta}{s}(T, \mu), \frac{\zeta}{s}(T, \mu), c_s(T), \alpha_s(T), etc.$

- ❖ v_2 and v_3 measurements in p-Au, d-Au and ^3He -Au @ 200 GeV by PHENIX

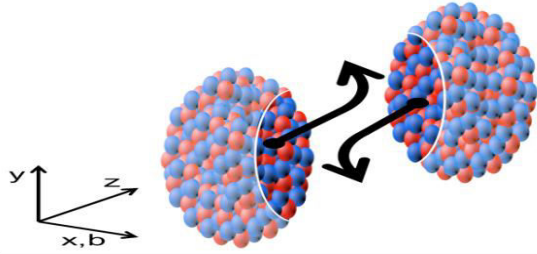
Nature Phys. 15 (2019) 3, 214-220



- ❖ Measurements demonstrate that the v_n 's are correlated to the initial geometry
- ❖ Hydrodynamic models, which include the formation of short-lived QGP droplets, provide a simultaneous description of these measurements

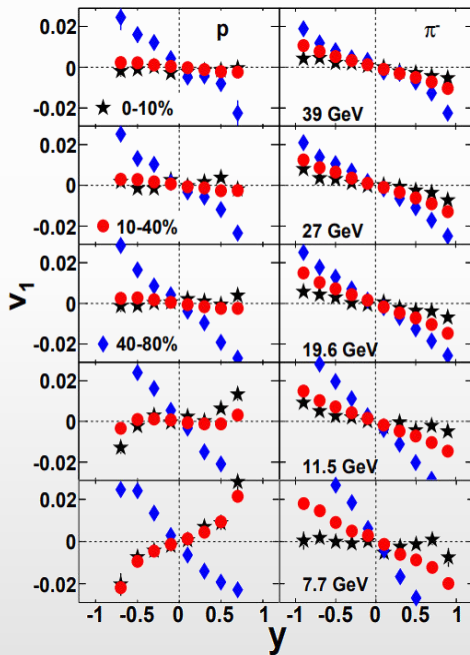


Flow at NICA energies



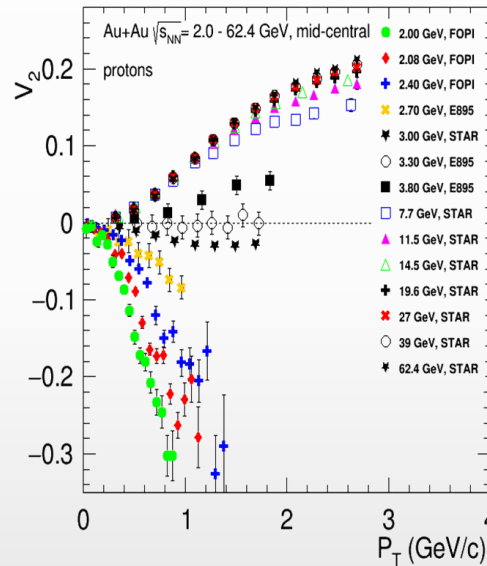
- ❖ Generated during the nuclear passage time $(2R/\gamma)$ – sensitive to EOS
 - ✓ RHIC @ 200 GeV $(2R/\gamma) \sim 0.1$ fm/c
 - ✓ AGS @ 3-4.5 GeV $(2R/\gamma) \sim 9-5$ fm/c

Phys.Rev.Lett. 112 (2014) 16, 162301



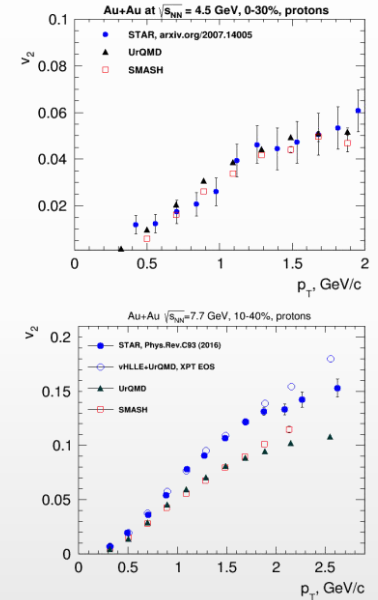
models do not reproduce measurements

EPJ Web Conf. 204 (2019) 03009



$\sqrt{s_{NN}} \sim 3-4.5$ GeV, pure hadronic models reproduce v_2 (JAM, UrQMD) \rightarrow degrees of freedom are the interacting baryons

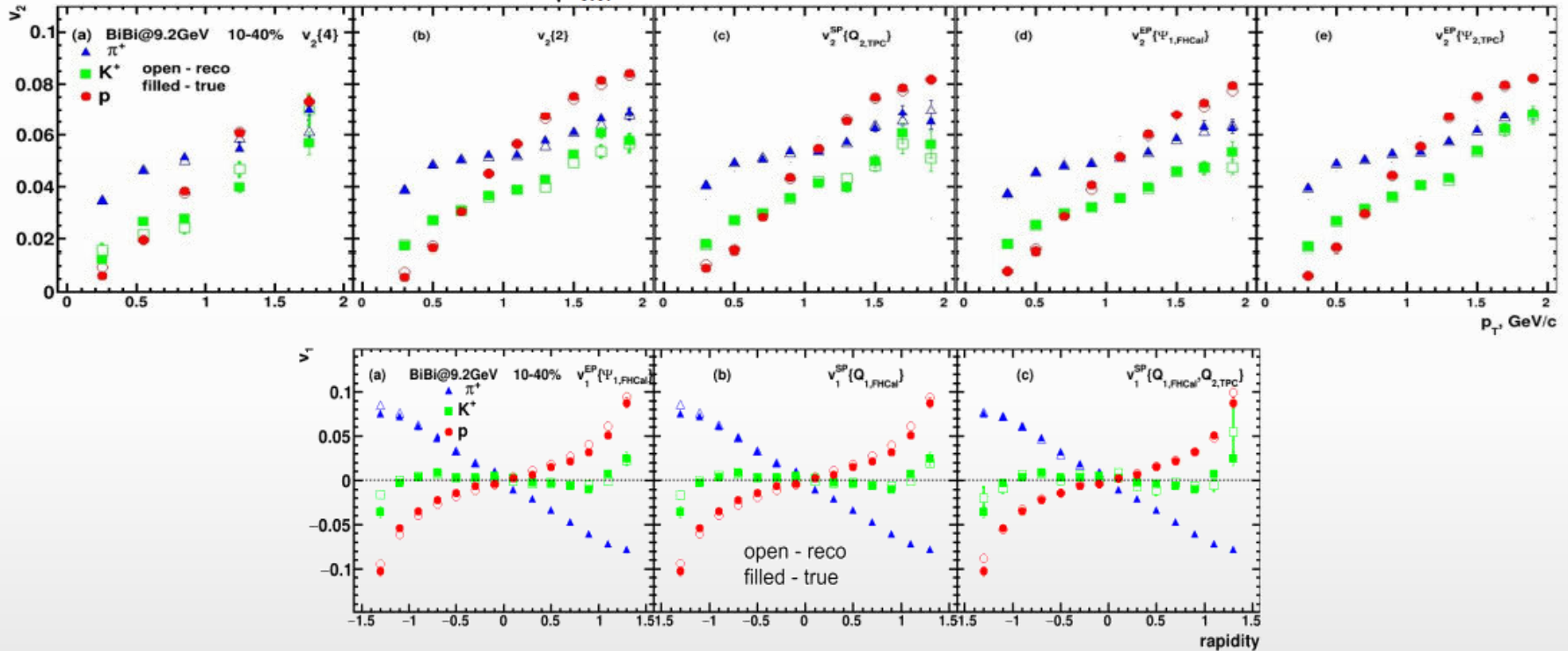
$\sqrt{s_{NN}} \geq 7.7$ GeV, need hybrid models with QGP phase (vHLL+UrQMD, AMPT with string melting,...)



- ❖ Flow is sensitive to fireball expansion and interactions with spectators
- ❖ Flow probes dominant degrees of freedom (hadronic vs. partonic)

❖ BiBi@9.2 GeV (UrQMD, 50M), full event reconstruction

UrQMD, Bi+Bi, $\sqrt{s_{NN}}=9.2$, 10-40%, reconstructed (GEANT4) – production 25

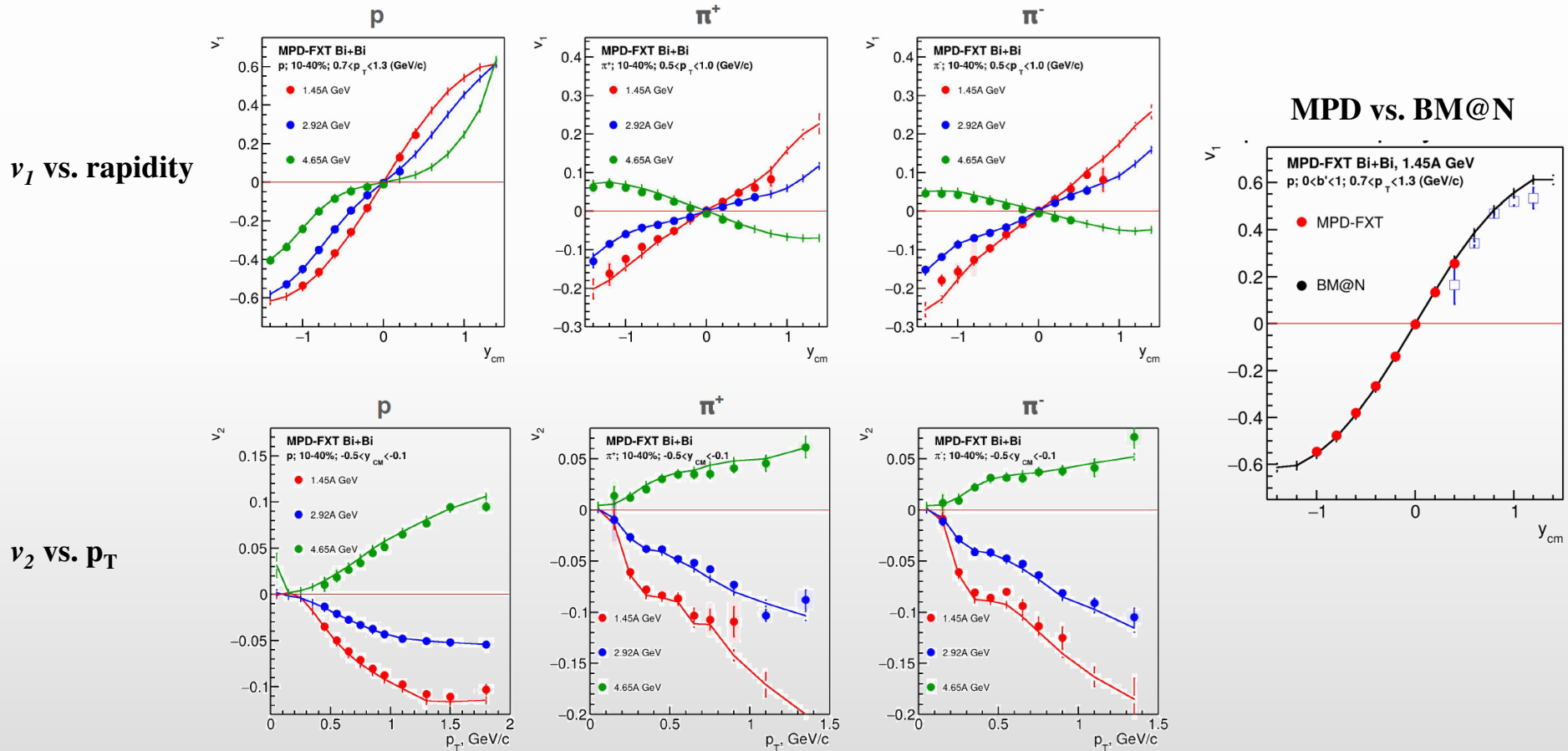


- Reconstructed and generated v_1 and v_2 for identified hadrons are in good agreement for all methods
- Measurements will be possible for weak decays of Ks, hyperons as well as short-lived resonances

NICA has capabilities to measure different flow harmonics for a wide variety of identified hadrons

System size scan for flow measurements is vital for understanding of the medium transport properties and onset of the phase transition → unique capability at NICA

- ❖ Request 33 mass production (UrQMD mean-field, fixed-target mode), BiBi @ 2.5, 3.0 and 3.5 GeV
- ❖ New: realistic PID (TPC+TOF); efficiency corrections; centrality by TPC multiplicity



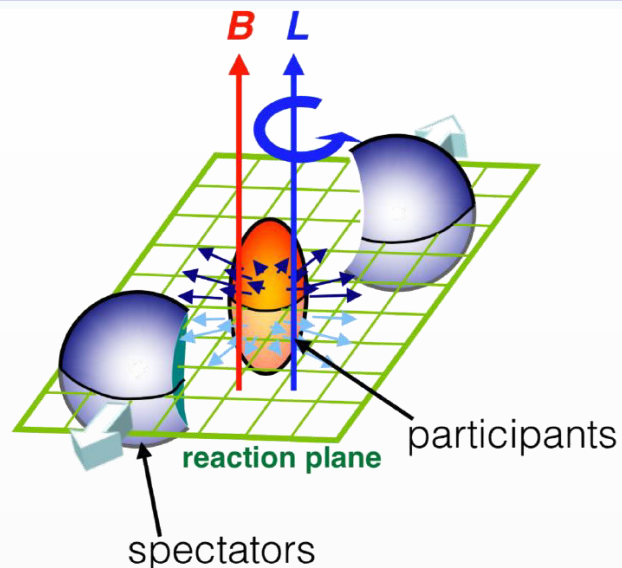
Reconstructed v_1 & v_2 are quantitatively consistent with truly generated signals
MPD and BM@N complete each other with modest overlap

initial state

QGP as a
relativistic
fluid

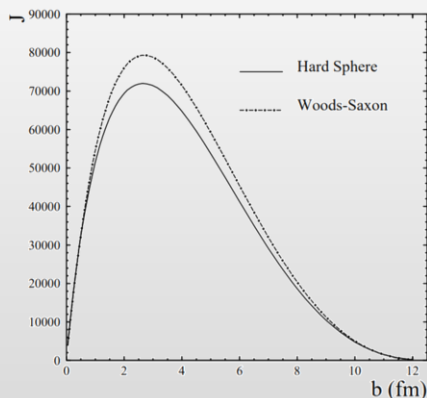
Global polarization of particles

Non-central heavy-ion collisions



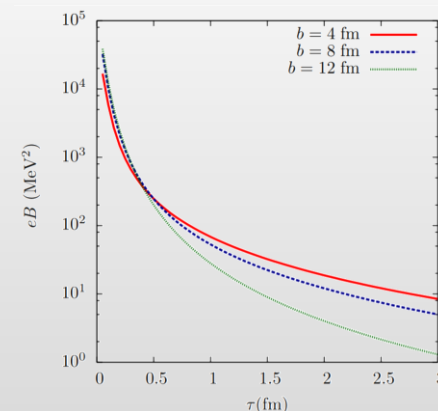
Large angular momentum due to medium rotations

Beccattini et al., PRC 77 (2008) 024906



Strong magnetic field ($\sim 10^{13}$ T) formed for a short period of time

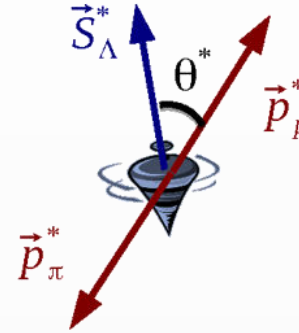
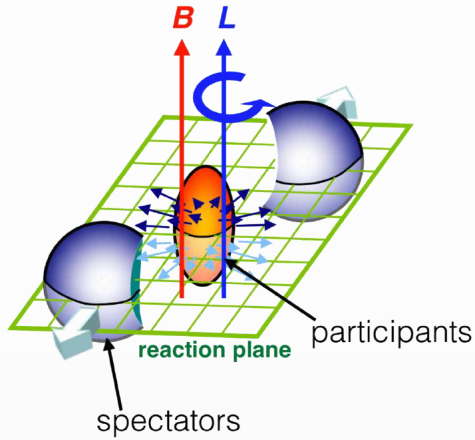
Kharzeev et al., NPA 803 (2008)



Focus is to see the effect of large angular momentum and magnetic field in heavy-ion collisions

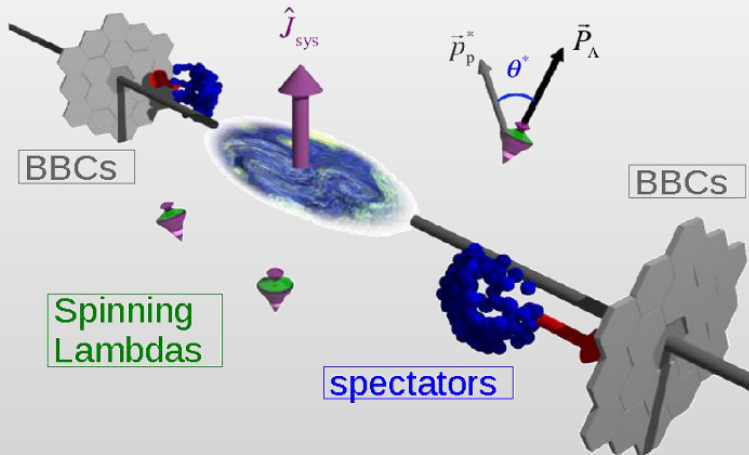
Global hyperon polarization

- ❖ Large angular momentum and strong magnetic field formed in mid-central heavy-ion collisions → polarization of particles in the final state



- ❖ $\Lambda/\bar{\Lambda}$ are “self-analyzing” probes → preferential emission of proton in spin direction

STAR, Nature 548, 62 (2017)



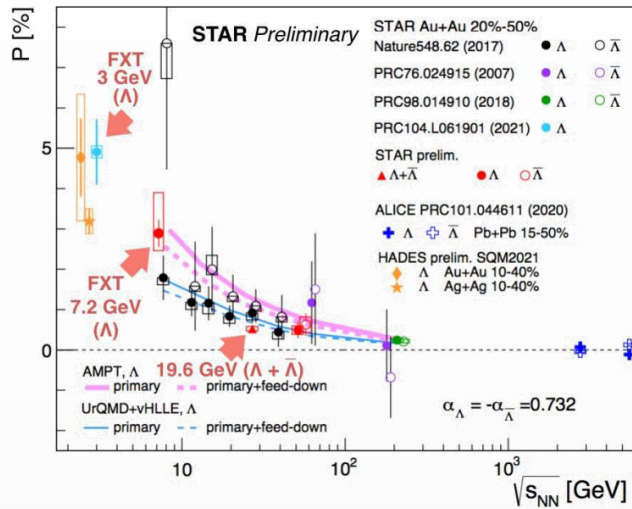
Phys.Rev.Lett.94:102301,2005;
Erratum-ibid.Lett.96:039901,2006

The global polarization observable is defined by [34](#):

$$P_{\Lambda} = \frac{8}{\pi\alpha_{\Lambda}} \frac{\langle \sin(\Psi_{EP} - \phi_p^*) \rangle}{R_{EP}}. \quad (1)$$

Here $\alpha_{\Lambda} = 0.732 \pm 0.014$ [35](#) is the Λ decay parameter, Ψ_{EP} the event plane angle, ϕ_p^* the azimuthal angle of the proton in the Λ rest frame, R_{EP} the resolution of the event plane angle and the brackets $\langle \cdot \rangle$ denote the average

❖ Global polarization of hyperons experimentally observed, decreases with $\sqrt{s_{NN}}$

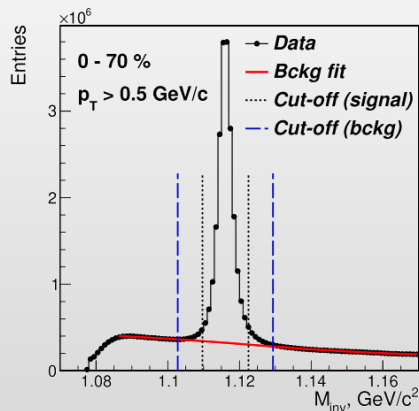


- ✓ reproduced by AMPT, 3FD, UrQMD+vHLLLE
- ✓ hint for a Λ - $\bar{\Lambda}$ difference, magnetic field:

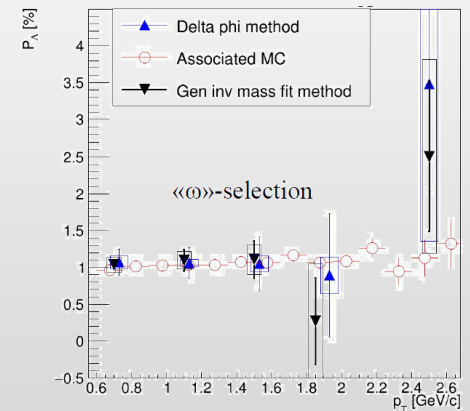
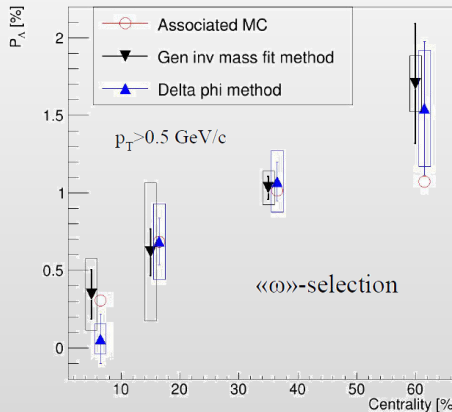
$$P_{\Lambda} \simeq \frac{1}{2} \frac{\omega}{T} + \frac{\mu_{\Lambda} B}{T} \quad P_{\bar{\Lambda}} \simeq \frac{1}{2} \frac{\omega}{T} - \frac{\mu_{\Lambda} B}{T}$$

NICA: extra points in the energy range 2-11 GeV centrality, p_T and rapidity dependence of polarization, not only for Λ , but other (anti)hyperons (Λ , Σ , Ξ)

❖ BiBi@9.2 GeV (PHSD), 15 M events \rightarrow full event reconstruction \rightarrow Λ global polarization

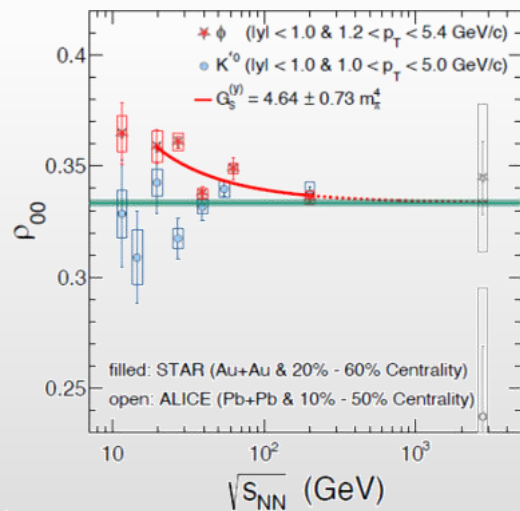
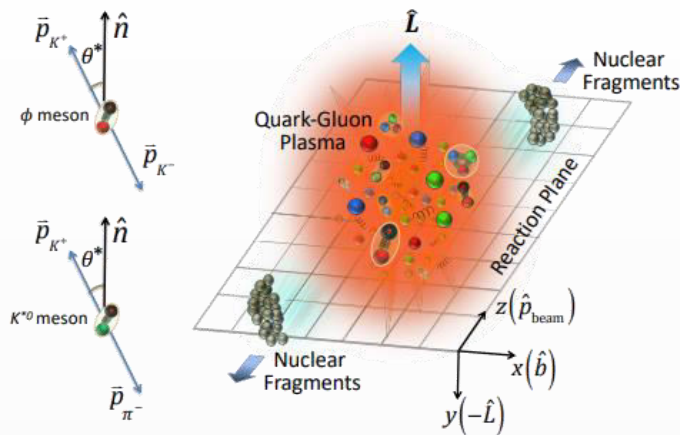


Performance study of the hyperon global polarization measurements with MPD at NICA, accepted to EPJA



First global polarization measurements for $\Lambda/\bar{\Lambda}$ will be possible with ~ 10 M data sampled events

Polarization of vector mesons: $K^*(892)$ and ϕ



- ❖ Light quarks can be polarized by $|\vec{J}|$ and $|\vec{B}|$
- ❖ If vector mesons are produced via recombination their spin may align
- ❖ Quantization axis:
 - ✓ normal to the production plane (momentum of the vector meson and the beam axis)
 - ✓ normal to the event plane (impact parameter and beam axis)
 - ✓ $\rho_{00}(\text{PP}) - \frac{1}{3} = [\rho_{00}(\text{EP}) - \frac{1}{3}] \left[\frac{1+3v_2}{4} \right]$
- ❖ Measured as anisotropies:

$$\frac{dN}{d\cos\theta} = N_0 \left[1 - \rho_{0,0} + \cos^2\theta (3\rho_{0,0} - 1) \right]$$

$\rho_{0,0}$ is a probability for vector meson to be in spin state = 0
 $\rightarrow \rho_{0,0} = 1/3$ corresponds to no spin alignment

- ❖ Measurements at RHIC/LHC challenge theoretical understanding $\rightarrow \rho_{00}$ can depend on multiple physics mechanisms (vorticity, magnetic field, hadronization scenarios, lifetimes and masses of the particles)

NICA: extend measurements in the NICA energy range, $\sqrt{s_{\text{NN}}} < 11$ GeV

initial state

QGP as a
relativistic
fluid

Hadronic resonances

Hadronic phase

- ❖ A phase between chemical and kinetic freeze out → lifetime and conditions?
- ❖ Short-lived resonances are sensitive to rescattering and regeneration in the hadronic phase

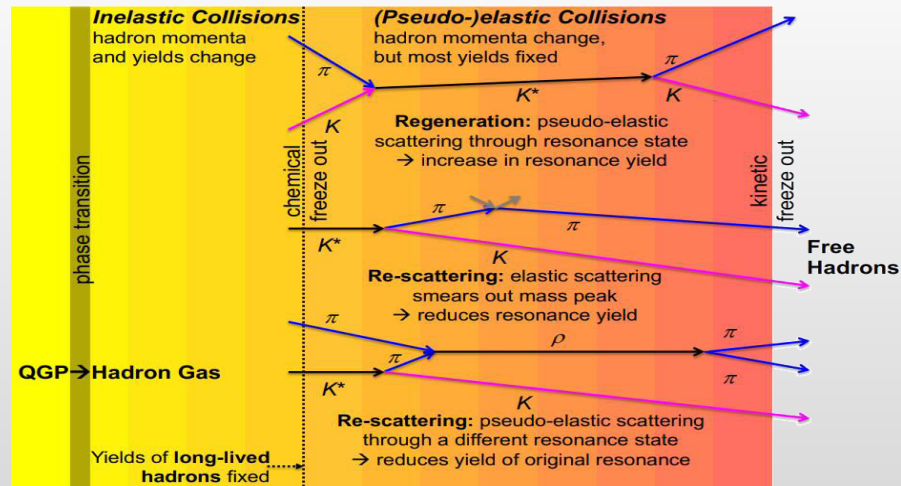
	$\rho(770)$	$K^*(892)$	$\Sigma(1385)$	$\Lambda(1520)$	$\Xi(1530)$	$\phi(1020)$
$c\tau$ (fm/c)	1.3	4.2	5.5	12.7	21.7	46.2
σ_{rescatt}	$\sigma_{\pi}\sigma_{\pi}$	$\sigma_{\pi}\sigma_K$	$\sigma_{\pi}\sigma_{\Lambda}$	$\sigma_K\sigma_p$	$\sigma_{\pi}\sigma_{\Xi}$	$\sigma_K\sigma_K$

- ❖ Reconstructed resonance yields in heavy ion collisions are defined by:

- ✓ resonance yields at chemical freeze-out
- ✓ hadronic processes between chemical and kinetic freeze-outs:

rescattering: daughter particles undergo elastic scattering or pseudo-elastic scattering through a different resonance → parent particle is not reconstructed → loss of signal

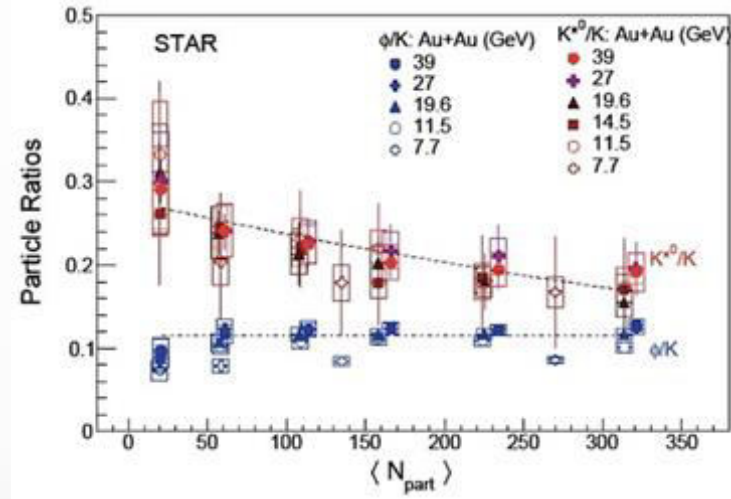
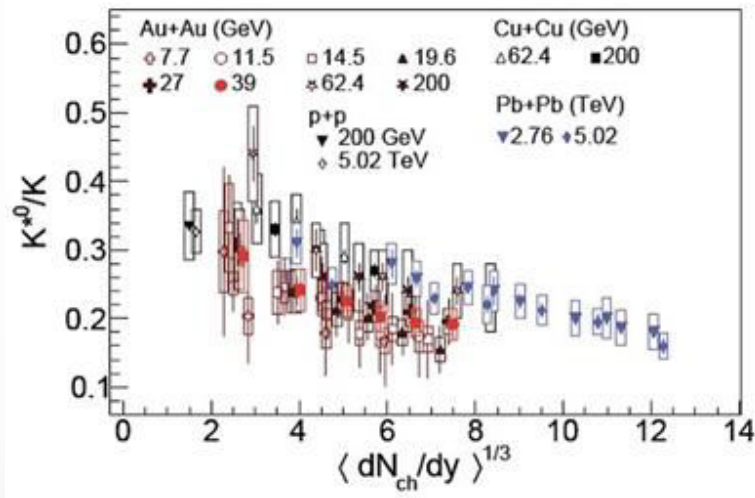
regeneration: pseudo-elastic scattering of decay products ($\pi K \rightarrow K^{*0}$, $KK \rightarrow \phi$ etc.) → increased yields



- ❖ Resonances provide the means to directly probe the hadronic phase properties

Experimental results

- ❖ Properties of the hadronic phase are studied by measuring ratios of resonance yields to yields of long-lived particles with same/similar quark contents: ρ/π , K^*/K , ϕ/K , Λ^*/Λ , $\Sigma^{*\pm}/\Sigma$ and Ξ^{*0}/Ξ

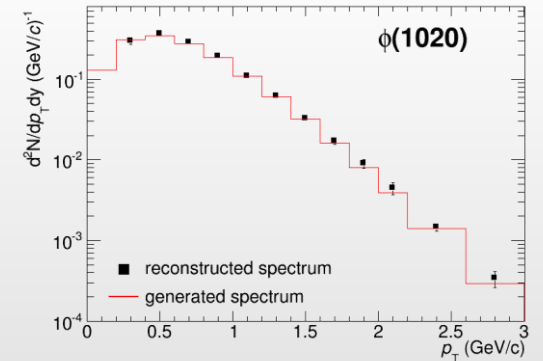
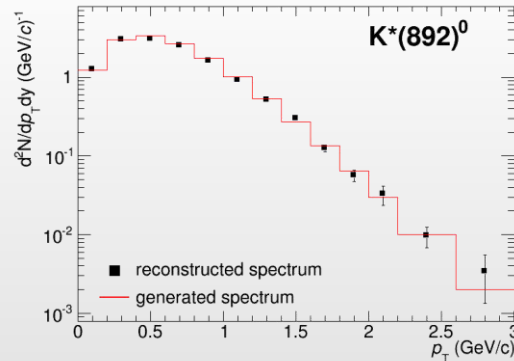
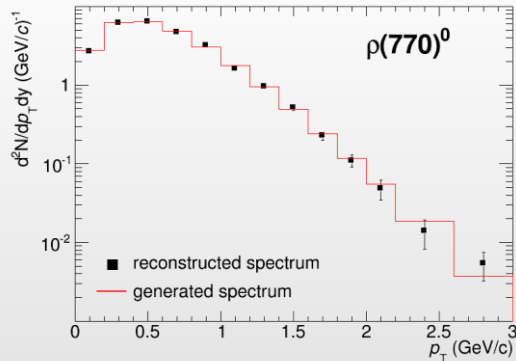
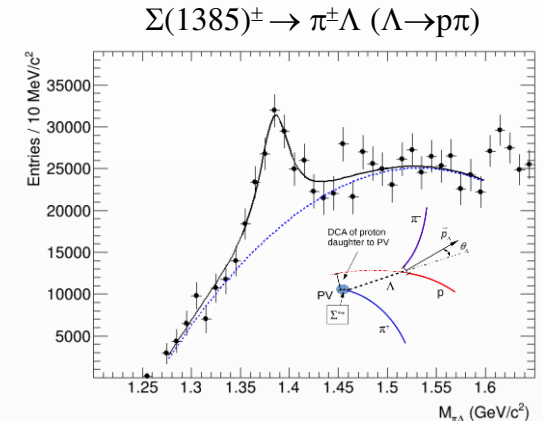
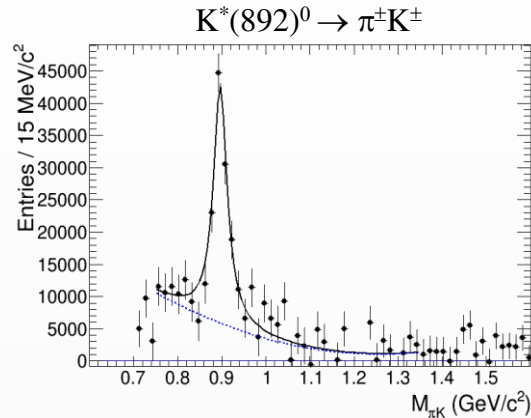
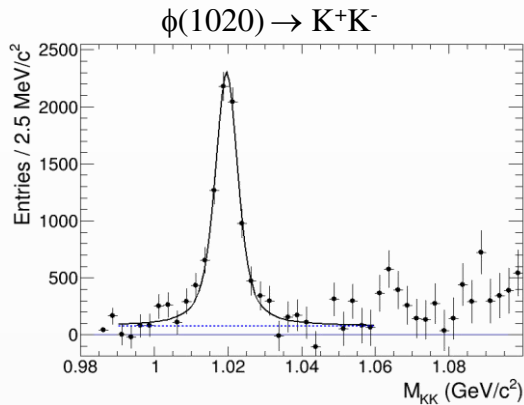


- ✓ suppressed production of short-lived resonances ($\tau < 20$ fm/c) in central A+A collisions \rightarrow rescattering takes over the regeneration
- ✓ no modification for longer-lived resonances, ϕ -meson ($\tau \sim 40$ fm/c)
- ✓ yield modifications depend on event multiplicity, not on collision system/energy
- ❖ Measurements in a wide energy range $\sqrt{s_{NN}} = 7$ -5000 GeV support the existence of a hadronic phase that lives long enough (up to $\tau \sim 10$ fm/c) to cause a significant reduction of the reconstructed yields of short-lived resonances
- ❖ All model predictions must be filtered through the hadronic phase

Precise measurements at NICA are needed to validate description of the hadronic phase in models

- ❖ BiBi@9.2 GeV (UrQMD) after mixed-event background subtraction, 10M events
- ❖ Examples of the low- p_T bins

Phys.Scripta 96 (2021) 6, 064002



MPD is capable of resonance reconstruction using h-ID in the TPC and TOF + topology selections for weak decays

First measurements are possible with 10M sampled events

initial state

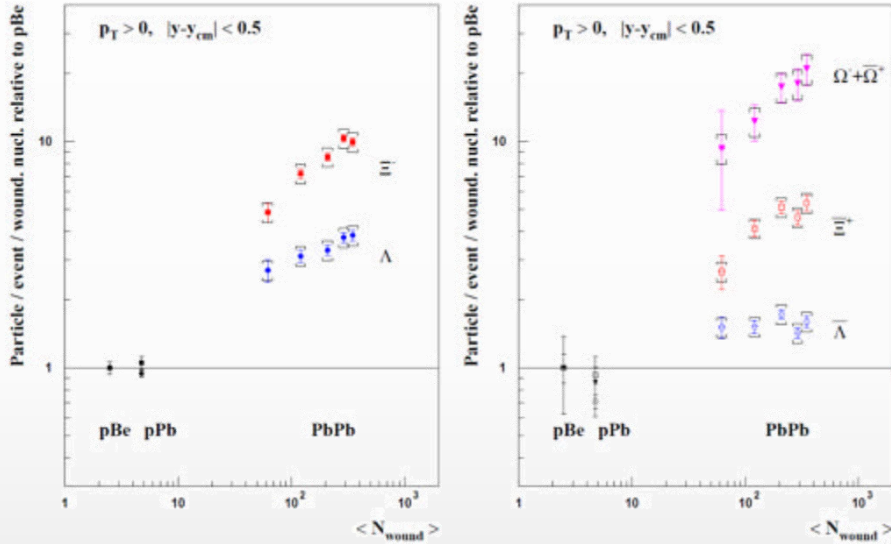
QGP as a
relativistic
fluid

Strangeness production

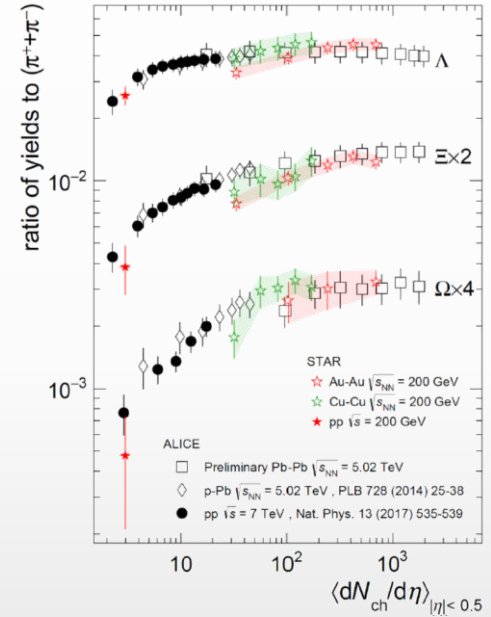
Strangeness production: pp, p-A, A-A

- ❖ Since the mid 80s, strangeness enhancement is considered as a signature of the QGP formation
- ❖ Experimentally observed in heavy-ion collisions at AGS, SPS, RHIC and LHC energies

NA57 and WA97 at SPS



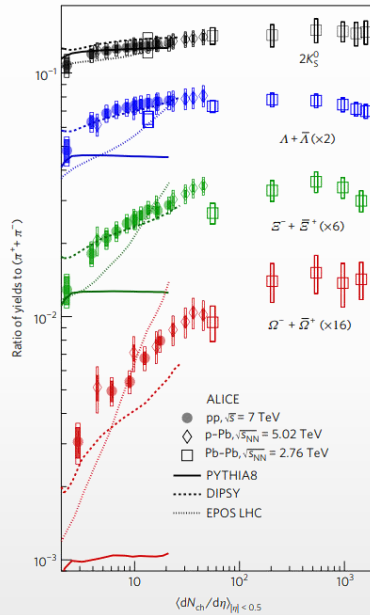
STAR at RHIC; ALICE at LHC



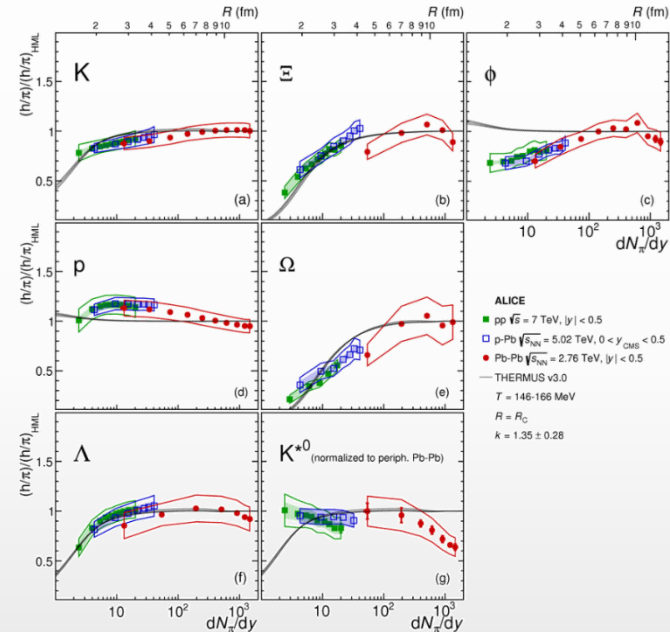
- ❖ Smooth evolution vs. multiplicity in pp, p-A and A-A collisions at LHC energies
- ❖ Strangeness enhancement increases with strangeness content and particle multiplicity
- ❖ STAR @ RHIC measurements in pp, A-A are in agreement with ALICE @ LHC at similar $\langle dN_{ch}/d\eta \rangle$
- ❖ Stronger relative enhancement at lower collision energies

- ❖ No consensus on the dominant strangeness enhancement mechanisms:
 - ✓ strangeness enhancement in QGP contradicts with the observed collision energy dependence
 - ✓ strangeness suppression in pp within canonical suppression models reproduces most of results except for $\phi(1020)$

Nature Physics volume 13, pages535–539 (2017)



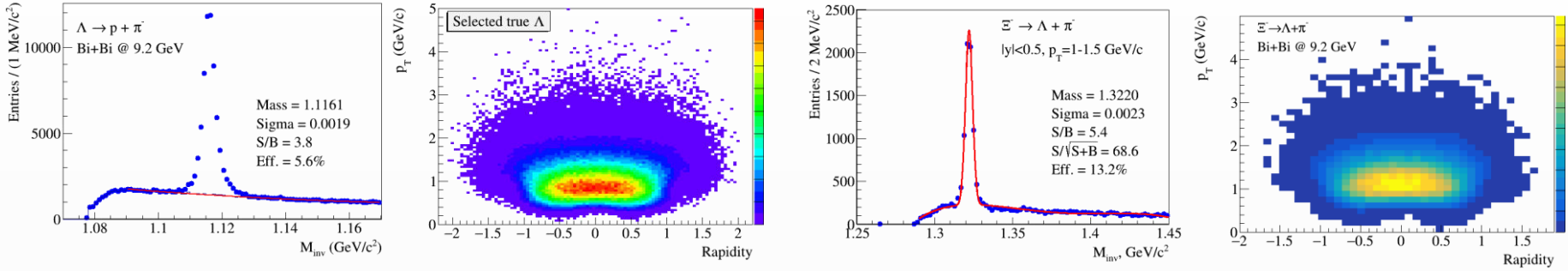
V. Vislavicius, A. Kalweit, arXiv:1610.03001



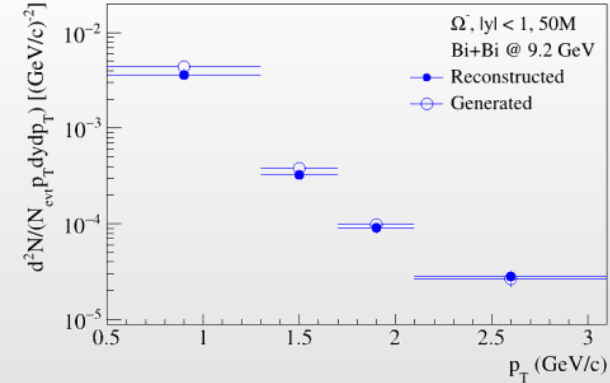
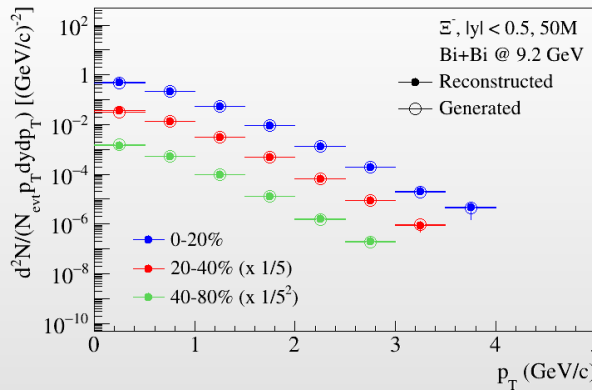
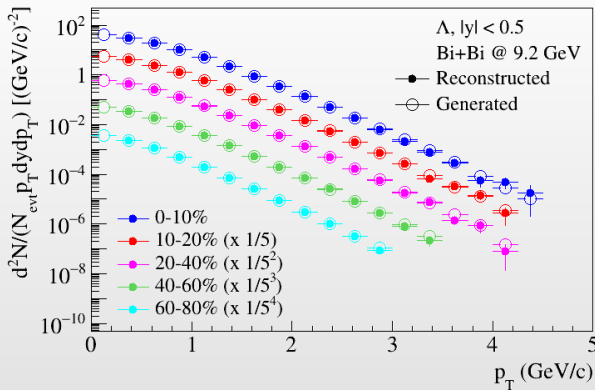
- ❖ System size scan for (multi)strange baryon and meson production in p+p, p+A and A+A collisions is a key to understanding of strangeness production:
 - ✓ excitation function of hadrons (yields, spectra, and ratios)
 - ✓ probe early stage and phase transformations in QCD medium, nuclear matter EOS and chemical equilibration

System size scan is unique capability of NICA in the energy range

❖ BiBi@9.2 GeV (UrQMD, 50M events), full event reconstruction



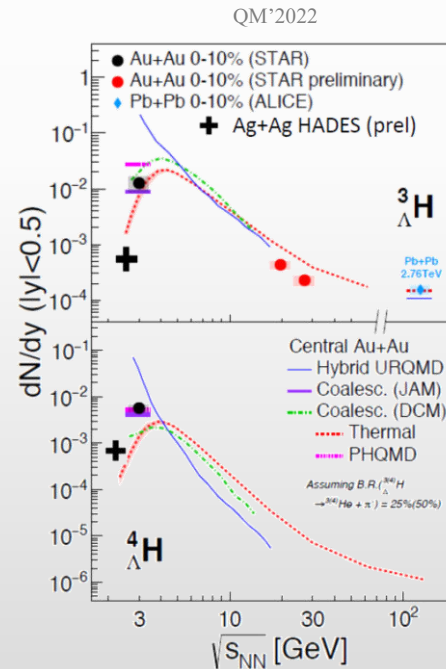
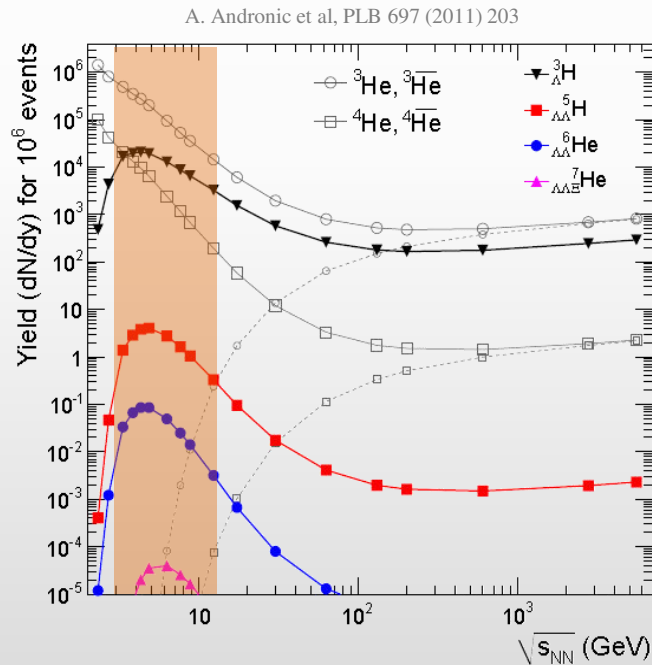
- different background estimates (fit function vs mixed-event)
- different PID selections for high- p_T daughter particles
- testing alternative Machine Learning techniques



MPD has capabilities to measure production of strange kaons, (multi)strange baryons and resonances in pp, p-A and A-A collisions using h-ID in the TPC&TOF and different decay topology selections

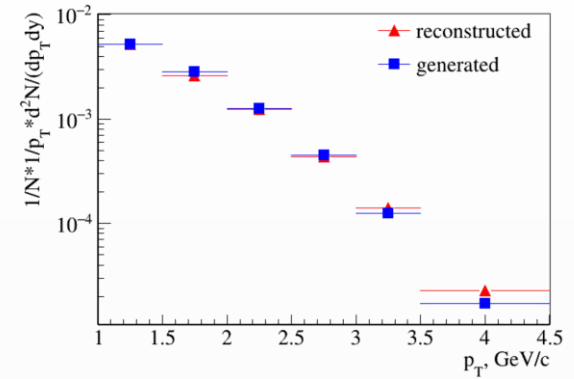
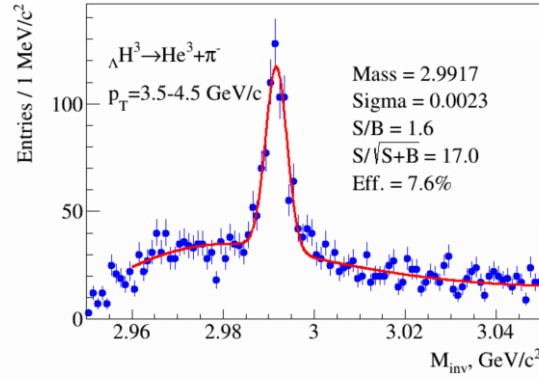
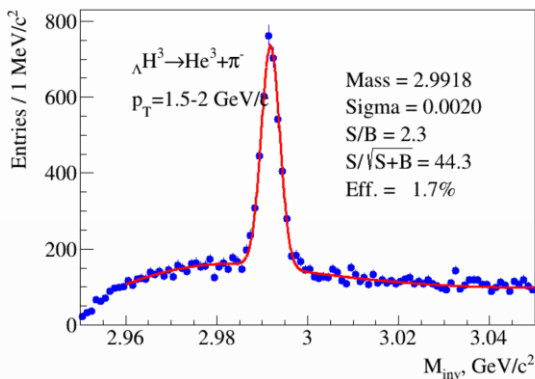
Light (hyper)nuclei

- Production mechanism usually described with two classes of phenomenological models :
 - ✓ statistical hadronization (SHM) \rightarrow production during phase transition, $dN/dy \propto \exp(-m/T_{\text{chem}})$
 - ✓ coalescence \rightarrow (anti)nucleons close in phase space ($\Delta p < p_0$) and matching the spin state form a nucleus
- Hypernuclei measurement studies are crucial:
 - ✓ microscopic production mechanism, Y-N (Y-Y, Y-N-N) potentials, strange sector of nuclear EoS
 - ✓ strong implications for astrophysical physics \rightarrow hyperons expected to exist in the inner core of neutron stars
- Models predict enhanced hypernuclei production at NICA \rightarrow double hypernuclei are reachable



Yields, lifetimes and binding energies are needed at NICA energies to provide tighter constraints

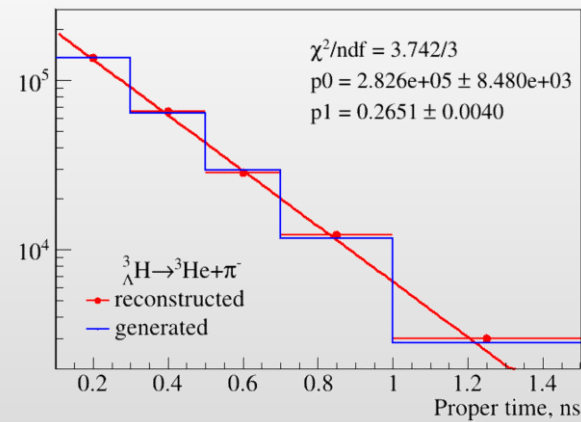
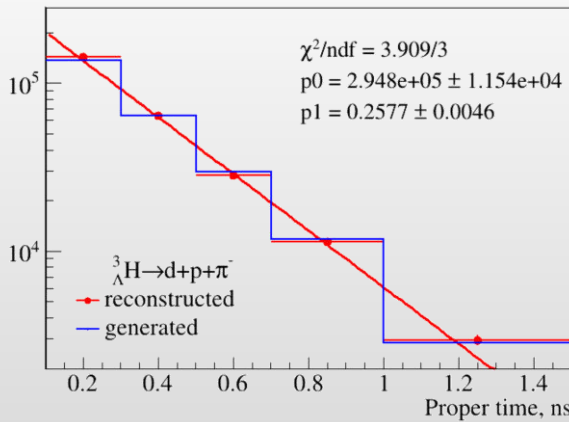
❖ Mass production 29 (PHQMD, BiBi@9.2 GeV, 40M events)



2- and 3-prong decay modes were studied separately to estimate systematics

$$N(\tau) = N(0) \exp\left(-\frac{\tau}{\tau_0}\right) = N(0) \exp\left(-\frac{ML}{cp\tau_0}\right)$$

Decay channel	Branching ratio	Decay channel	Branching ratio
$\pi^- + {}^3He$	24.7%	$\pi^- + p + p + n$	1.5%
$\pi^0 + {}^3H$	12.4%	$\pi^0 + n + n + p$	0.8%
$\pi^- + p + d$	36.7%	$d + n$	0.2%
$\pi^0 + n + d$	18.4%	$p + n + n$	1.5%



ΛH^3 reconstruction with ~ 50M samples events
 $\Lambda H^4, \Lambda He^4$ reconstruction with ~ 150M samples events

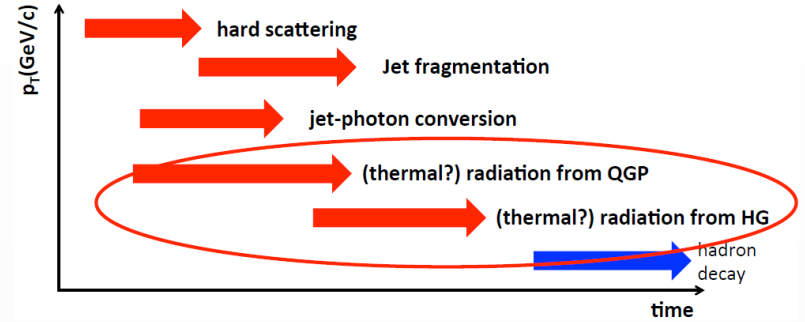
initial state

QFT as a
relativistic
fluid

Electromagnetic radiation

Direct photons and system temperature

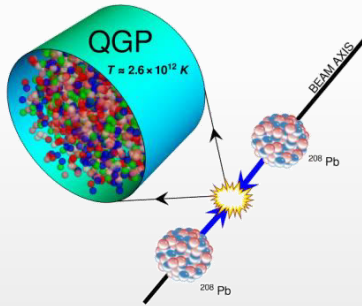
- Direct photons are all photons except for those coming from hadron decays:
 - ✓ produced during all stages of the collision
 - ✓ QGP is transparent for photons → penetrating probe



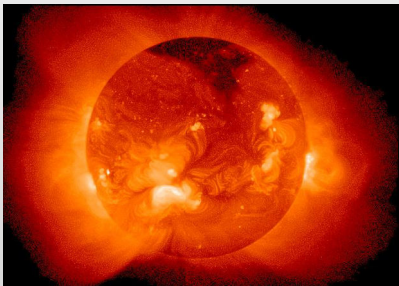
- Low-E photons → effective temperature of the system:

$$E_\gamma \frac{d^3 N_\gamma}{d^3 p_\gamma} \propto e^{-E_\gamma / T_{\text{eff}}}$$

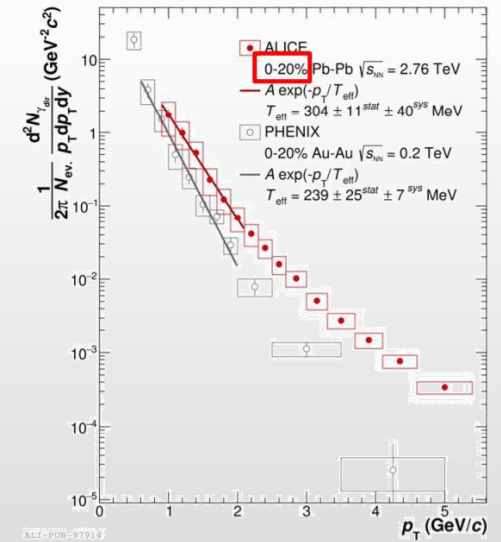
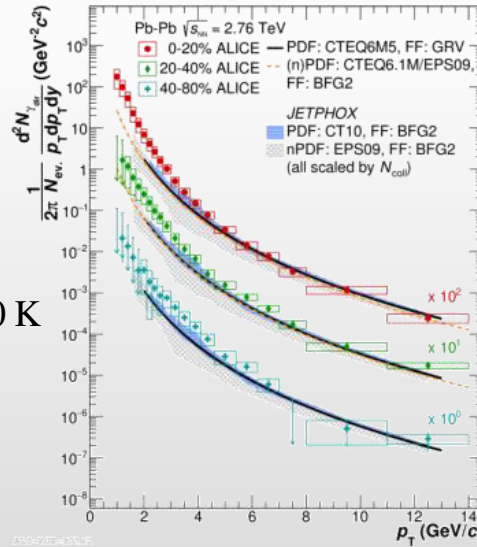
- Relativistic A+A collisions → the highest temperature created in laboratory ~ 10¹² K



Temperature at the center of the Sun ~ 15 000 000 K



A medium of ~ 200 MeV is 100 000 times hotter !!!

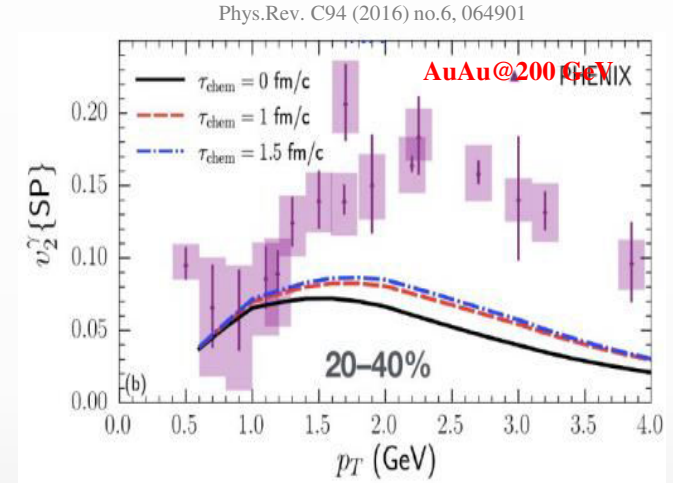
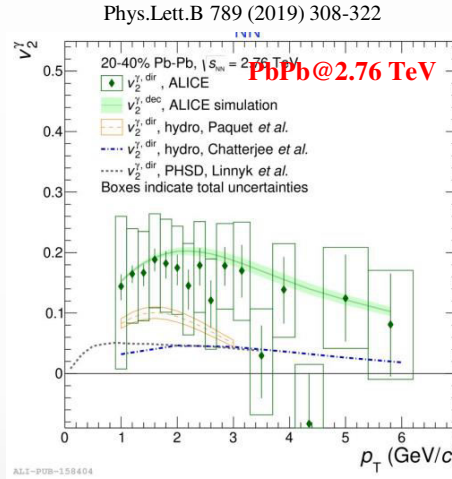
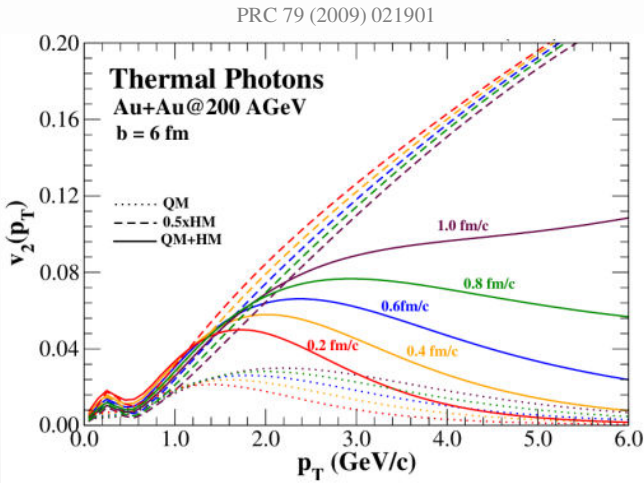


$T_{\text{eff}} \sim 240$ MeV at RHIC; $T_{\text{eff}} \sim 300$ MeV at the LHC

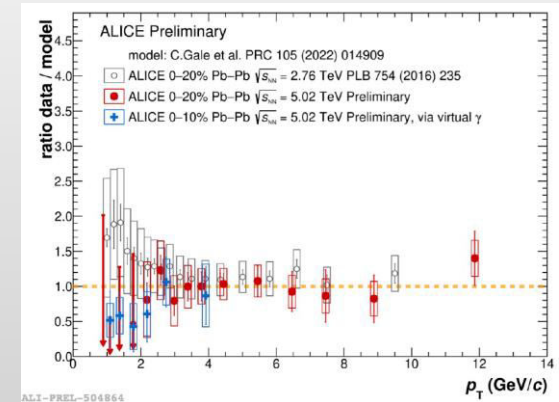
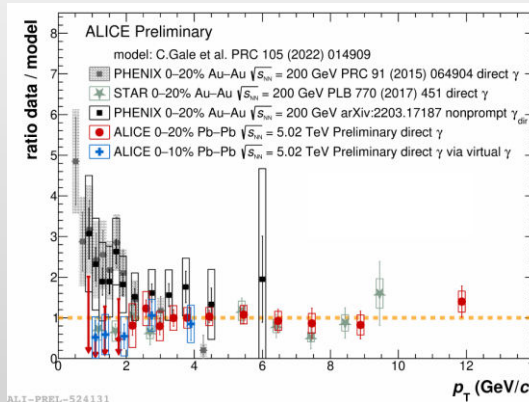
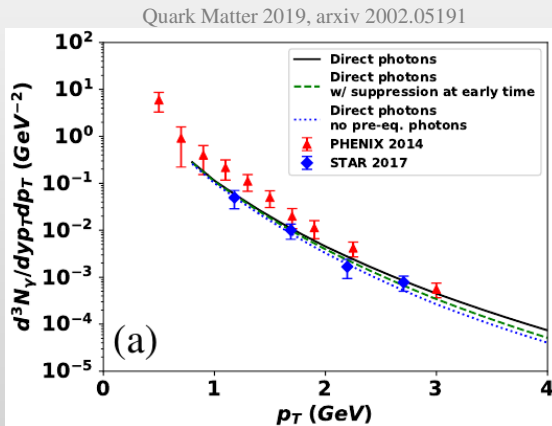
$T_{\text{eff}} \gg T_c \sim 150$ MeV predicted by LQCD

Direct photons puzzle(s)

- ❖ Simultaneous description of direct photon yields and elliptic flow (v_2) is problematic:
 - ✓ direct photon flow is similar to flow of decay photons, underestimated by hydro \rightarrow favors late emission
 - ✓ large yields of low-E direct photon yields require early emission in to be described by hydro models



- ❖ Controversial results reported for different systems by different experiments



Expectations for NICA

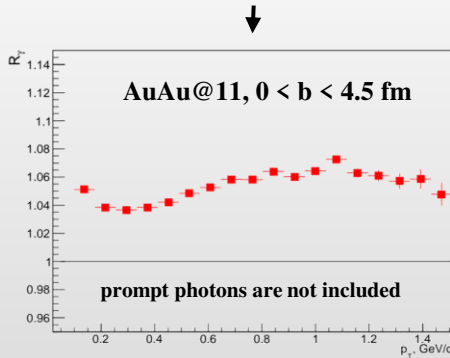
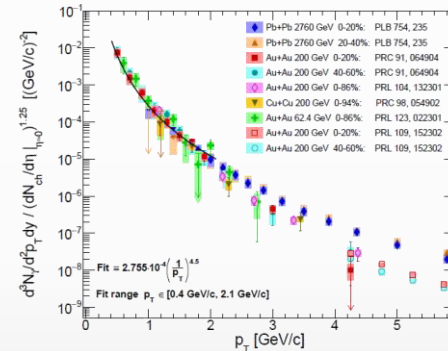
- Experimental measurements in A+A collisions are available from the LHC (2.76-5 TeV), RHIC (62-200 GeV) and WA98 (17.2 GeV)
- No measurements at NICA energies (direct photon yields and flow vs. p_T and centrality)

Estimation of the direct photon yields @NICA

model calculations

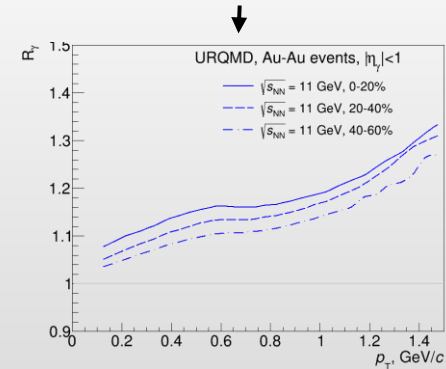
empirical scaling

- UrQMD v3.4 with hybrid model (3+1D hydro, bag model EoS, hadronic rescattering and resonances within UrQMD)
- Each cell have T_i, E_i, μ_{bi} :
 - T is high – QGP phase (Peter Arnold, Guy D. Moore, Laurence G. Yaffe, JHEP 0112:009 2001)
 - T is low – HG phase (Simon Turbide, Ralf Rapp, Charles Gale, Phys.Rev.C69:014903,2004)
 - T is intermediate – mixed phase
- Integrate over all cells and all time steps
- Calculations reproduce hydro calculations for the SPS



$$R_\gamma = \frac{\gamma_{inc}}{\gamma_{decay}} = \frac{\gamma_{inc}/\pi^0}{\gamma_{decay}/\pi^0_{param}}$$

$$\gamma_{direct} = \left(1 - \frac{1}{R_\gamma}\right) \cdot \gamma_{inc}$$



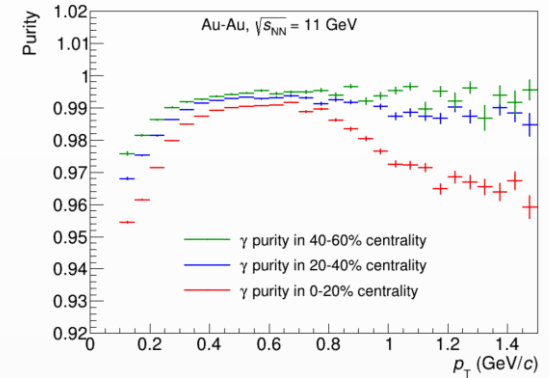
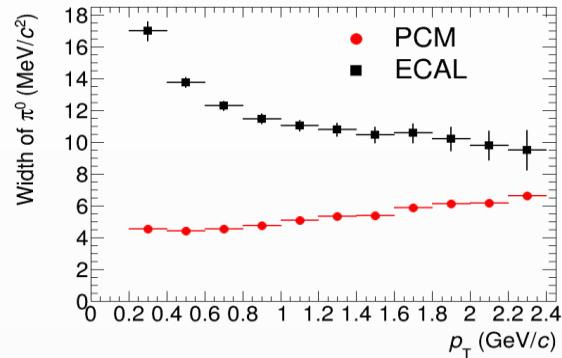
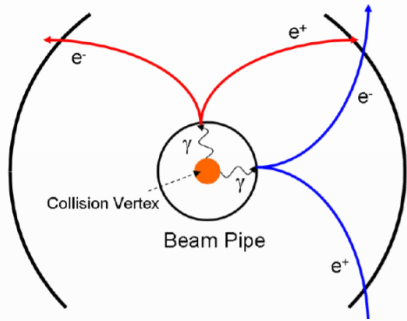
- Non-zero direct photon yields are predicted, $R_\gamma \sim 1.05 - 1.15 \rightarrow$ experimentally reachable by MPD!!!

Potentially, NICA can provide unique measurements for direct photons in the NICA energy range

Prospects for the MPD

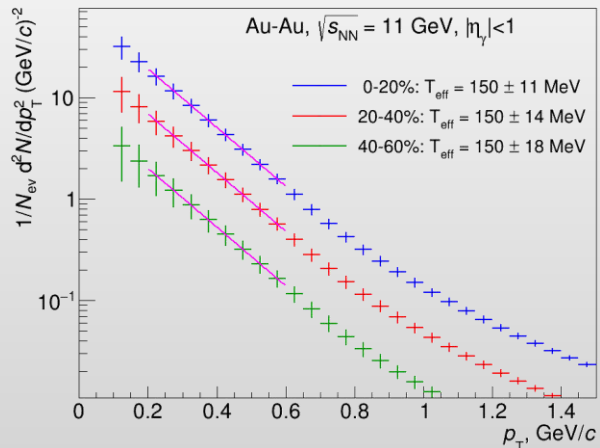
- ❖ Photons can be measured in the ECAL or in the tracking system as e^+e^- conversion pairs (PCM)

beam pipe (0.3% X_0) + inner TPC vessels (2.4% X_0)



- ❖ Main sources of systematic uncertainties for direct photons:

- ✓ detector material budget \rightarrow conversion probability
- ✓ π^0 reconstruction efficiency
- ✓ p_T -shapes of π^0 and η production spectra

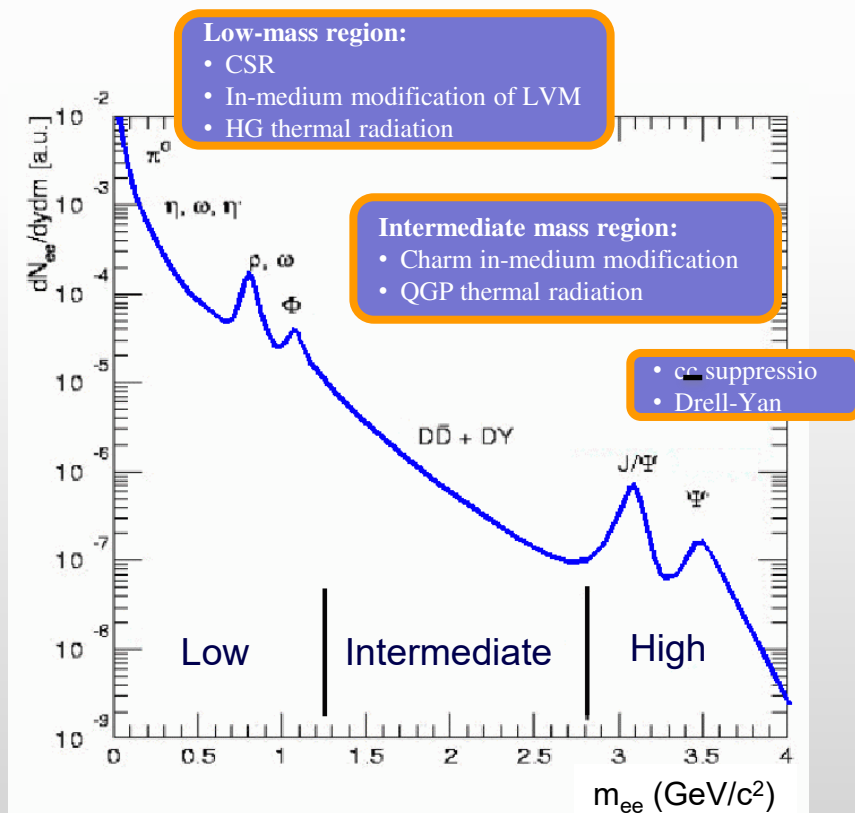


- ✓ ECAL and PCM for photon reconstruction and measurement of neutral mesons (background)
- ✓ With $R_\gamma \sim 1.1$ and $\delta R_\gamma/R_\gamma \sim 3\%$ \rightarrow uncertainty of $T_{\text{eff}} \sim 10\%$
- ✓ Development of reconstruction techniques and estimation of needed statistics are in progress

\rightarrow potentially, MPD can provide unique measurements for direct photon production in the NICA energy range

Dielectron continuum and LVMs

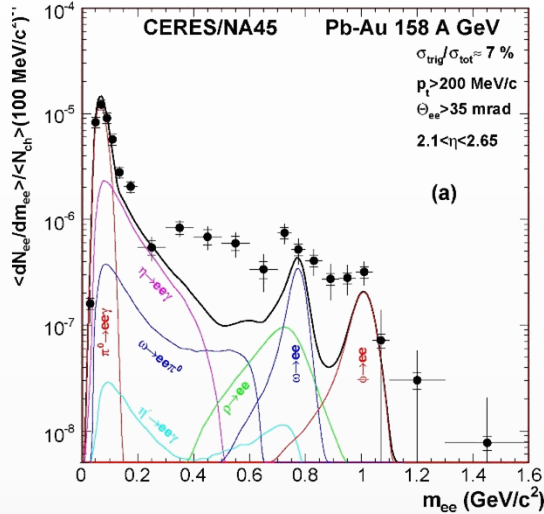
- The QCD matter produced in A-A interactions is transparent for leptons, once produced they leave the interaction region largely unaffected + not sensitive to collective expansion
- Dielectron continuum at low and intermediate mass/ p_T carries a wealth of information about reaction dynamics and medium properties:
 - ✓ low-mass part sensitive to late (hadronic) stage, intermediate mass — to hot stage
 - ✓ ρ -meson peak: modification of ρ -meson properties in hot matter (chiral phase transition)
 - ✓ charm production and correlations etc.



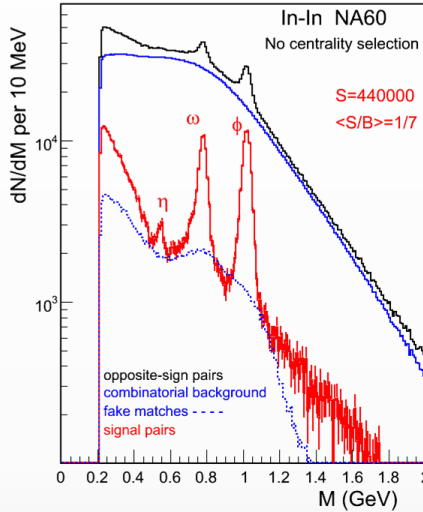
i	Dilepton channels	
1	Dalitz decay of π^0 :	$\pi^0 \rightarrow \gamma e^+ e^-$
2	Dalitz decay of η :	$\eta \rightarrow \gamma l^+ l^-$
3	Dalitz decay of ω :	$\omega \rightarrow \pi^0 l^+ l^-$
4	Dalitz decay of Δ :	$\Delta \rightarrow N l^+ l^-$
5	Direct decay of ω :	$\omega \rightarrow l^+ l^-$
6	Direct decay of ρ :	$\rho \rightarrow l^+ l^-$
7	Direct decay of ϕ :	$\phi \rightarrow l^+ l^-$
8	Direct decay of J/Ψ :	$J/\Psi \rightarrow l^+ l^-$
9	Direct decay of Ψ' :	$\Psi' \rightarrow l^+ l^-$
10	Dalitz decay of η' :	$\eta' \rightarrow \gamma l^+ l^-$
11	pn bremsstrahlung:	$pn \rightarrow p n l^+ l^-$
12	$\pi^\pm N$ bremsstrahlung:	$\pi^\pm N \rightarrow \pi N l^+ l^-$

Experimental measurements

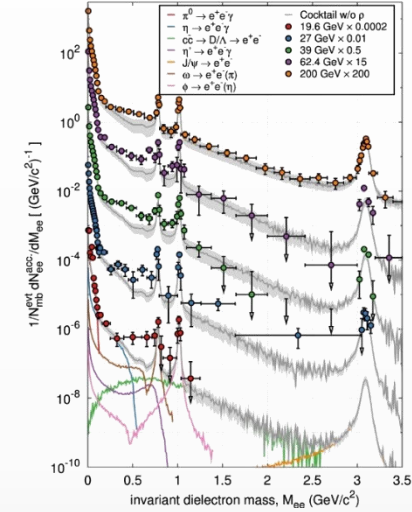
Last CERES result
PLB 666 (2008) 425



In+In 158 A GeV
PRL 96, 162302 (2006)



BES @ RHIC
PRL 113, 22301 (2014); PRC 92, 24912 (2015)



❖ A-A systems at all energies studied show:

- ✓ LMR: clear enhancement of dileptons wrt to known hadronic sources \rightarrow HG thermal radiation, broadening of ρ spectral shape
- ✓ IMR: no clear picture, uncertainties for charm production

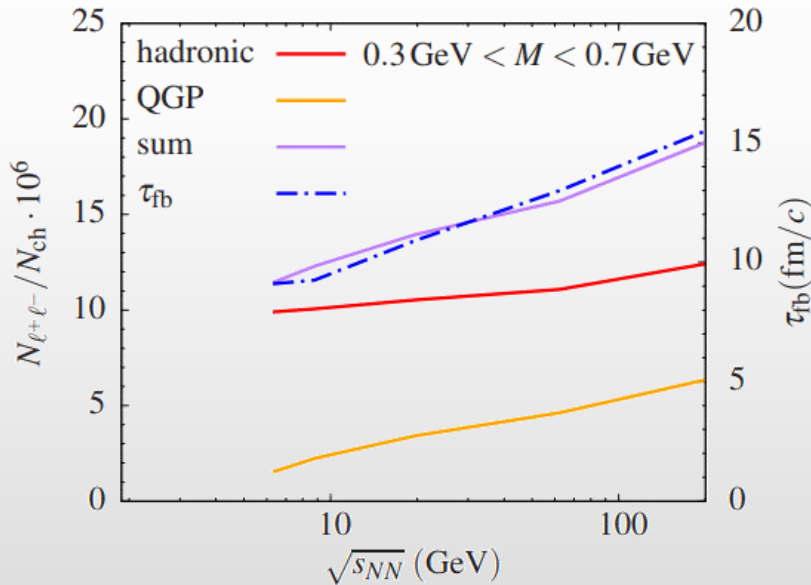
❖ Dilepton excess is consistently reproduced by microscopic many body model (Rapp et al.)

Prospects

- Onset of deconfinement? Onset of CSR? Energy scan of dilepton excess:
 - Integrated yield in the LMR tracks the fireball lifetime
 - Inverse slope of the mass spectrum in the IMR provides a measurement of $\langle T \rangle$, no blue shift
 - First order phase transition, “anomalous” variations in the fireball lifetime related to critical phenomena.?
 - Thermal radiation down to $\sqrt{s_{NN}} = 6$ GeV ?

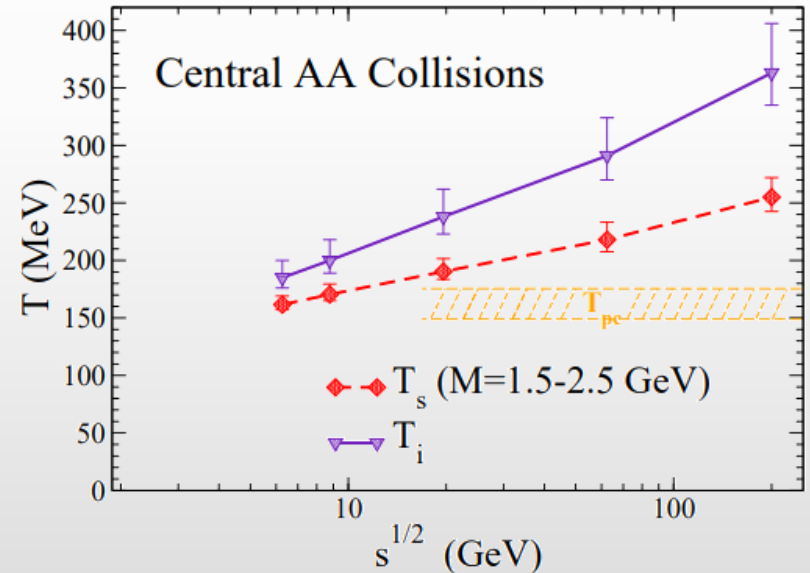
LMR as chronometer

PLB 753, 586 (2016)



Integrated thermal excess radiation tracks the total fireball lifetime within $\sim 10\%$ \rightarrow non-monotonous lifetime variations trace critical phenomena

IMR as thermometer

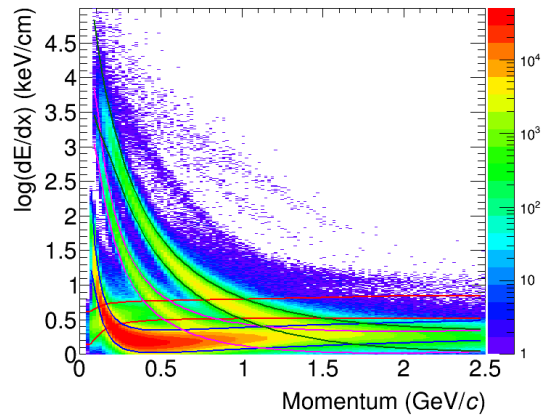


$dR_{ll}/dM \propto (MT)^{3/2} \exp(-M/T_s)$
 T_s smoothly evolves $T = 160$ MeV to 260 MeV
 Measured T_s is 15-30% below the initial T_i

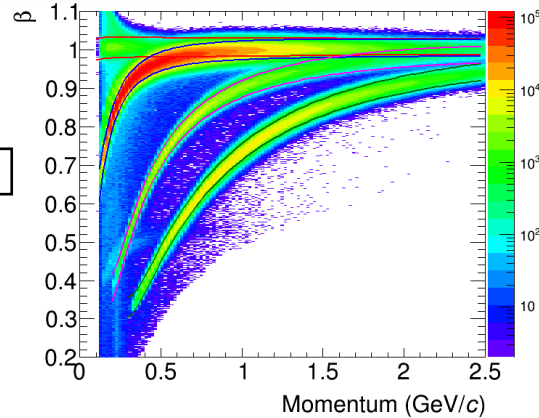
e-ID with MPD

❖ eID with TPC + TOF

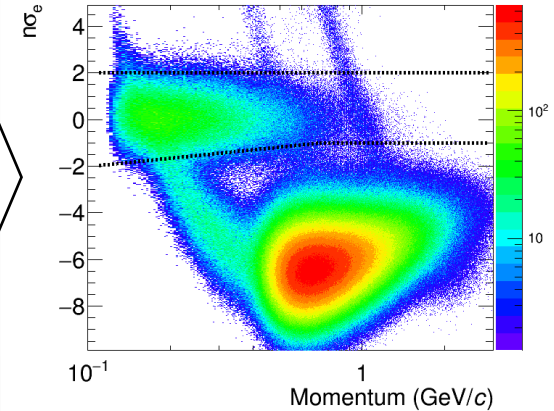
n-sigma dE/dx parameterization



n-sigma β -TOF parameterization

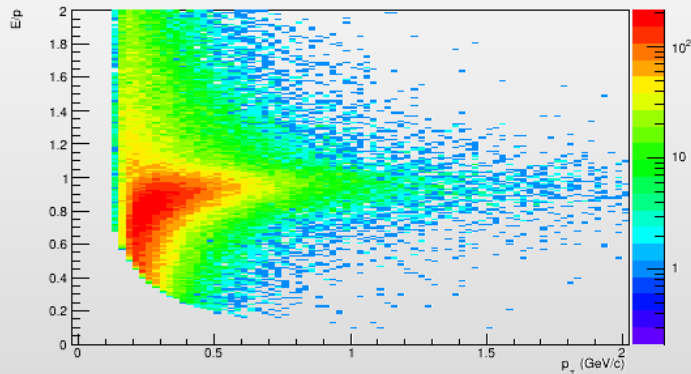


n- σ dE/dx distribution for tracks matched to TOF and identified as electrons



❖ eID with ECAL

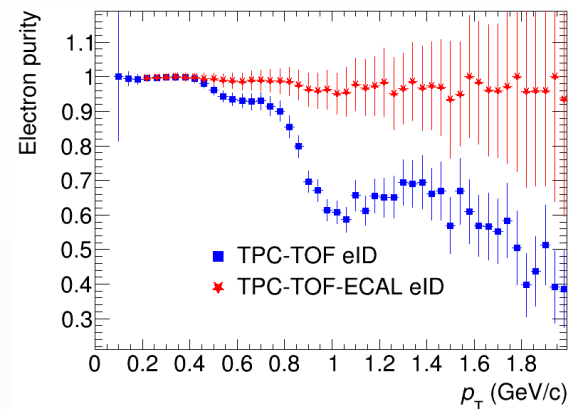
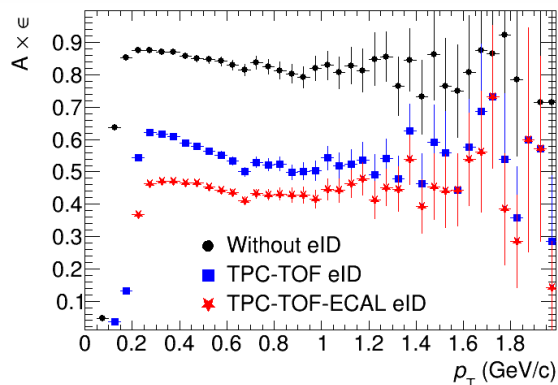
E/p for electron tracks



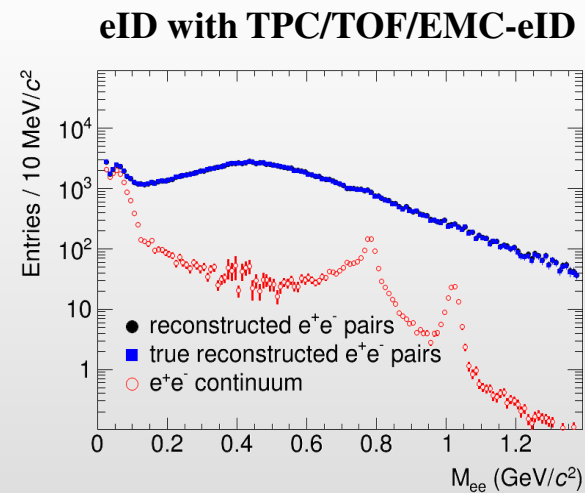
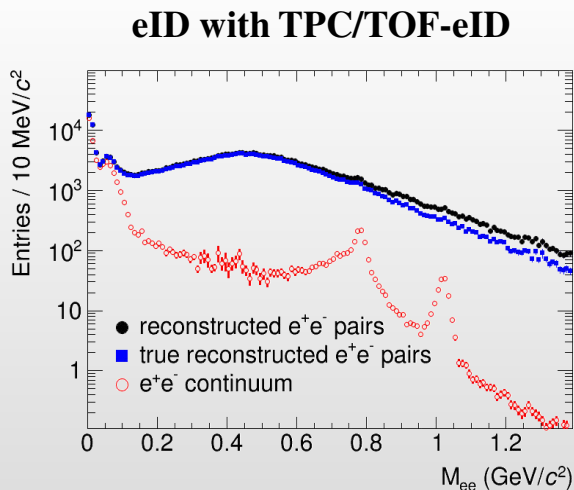
- ECAL e-ID for 2σ -matched tracks:
 - ✓ TOF < 2 ns ($\delta \sim 500$ ps)
 - ✓ $E/p \sim 1$
- Turns on at $p_T > 200$ MeV/c

Electrons and dielectron spectra

- ❖ Electron reconstruction efficiency and purity, AuAu@11 (UrMQD v.3.4) events



- ❖ Dielectron continuum



- ❖ MPD provides reconstruction of electrons with high purity
- ❖ S/B for dielectron measurements was achieved at 1/20 in the mass region 0.2-1.4 MeV/c²

Multi-Purpose Detector (MPD) Collaboration



MPD International Collaboration was established in 2018 to construct, commission and operate the detector

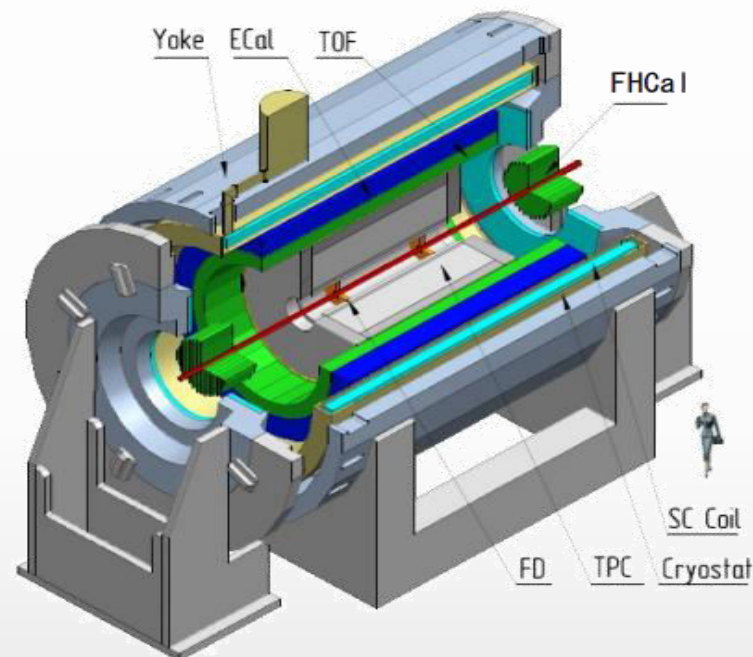
12 Countries, >500 participants, 38 Institutes and JINR

Organization

Acting Spokesperson: **Victor Riabov**
Deputy Spokespersons: **Zebo Tang, Arkadiy Taranenko**
Institutional Board Chair: **Alejandro Ayala**
Project Manager: **Slava Golovatyuk**

Joint Institute for Nuclear Research, Dubna;

*A. Alikhanyan National Lab of Armenia, Yerevan, **Armenia**;*
*SSI "Joint Institute for Energy and Nuclear Research – Sosny" of the National Academy of Sciences of Belarus, Minsk, **Belarus***
*University of Plovdiv, **Bulgaria**;*
*Tsinghua University, Beijing, **China**;*
*University of Science and Technology of China, Hefei, **China**;*
*Huzhou University, Huzhou, **China**;*
*Institute of Nuclear and Applied Physics, CAS, Shanghai, **China**;*
*Central China Normal University, **China**;*
*Shandong University, Shandong, **China**;*
*University of Chinese Academy of Sciences, Beijing, **China**;*
*University of South China, **China**;*
*Three Gorges University, **China**;*
*Institute of Modern Physics of CAS, Lanzhou, **China**;*
*Tbilisi State University, Tbilisi, **Georgia**;*
*Institute of Physics and Technology, Almaty, **Kazakhstan**;*
*Benemérita Universidad Autónoma de Puebla, **Mexico**;*
*Centro de Investigación y de Estudios Avanzados, **Mexico**;*
*Instituto de Ciencias Nucleares, UNAM, **Mexico**;*
*Universidad Autónoma de Sinaloa, **Mexico**;*
*Universidad de Colima, **Mexico**;*
*Universidad de Sonora, **Mexico**;*
*Universidad Michoacana de San Nicolás de Hidalgo, **Mexico***
*Institute of Applied Physics, Chisinev, **Moldova**;*
*Institute of Physics and Technology, **Mongolia**;*



*Belgorod National Research University, **Russia**;*
*Institute for Nuclear Research of the RAS, Moscow, **Russia**;*
*High School of Economics University, Moscow, **Russia***
*National Research Nuclear University MEPhI, Moscow, **Russia**;*
*Moscow Institute of Science and Technology, **Russia**;*
*North Osetian State University, **Russia**;*
*National Research Center "Kurchatov Institute", **Russia**;*
*Peter the Great St. Petersburg Polytechnic University Saint Petersburg, **Russia**;*
*Plekhanov Russian University of Economics, Moscow, **Russia**;*
*St. Petersburg State University, **Russia**;*
*Skobeltsyn Institute of Nuclear Physics, Moscow, **Russia**;*
*Petersburg Nuclear Physics Institute, Gatchina, **Russia**;*
*Vinča Institute of Nuclear Sciences, **Serbia**;*
*Pavol Jozef Šafárik University, Košice, **Slovakia***



MPD Collaboration meeting in JINR (Dubna): April 23-25



- ❖ Heavy-ion collisions provide the means to study QCD phase diagram at extreme conditions (T, μ)
- ❖ Heavy-ion collisions are studied for over 30 years now, however, there is still a lot to be understood
- ❖ MPD@NICA is in final stage of preparation \rightarrow QCD matter at maximum (net)baryon densities
- ❖ MPD@NICA provides capabilities for important/unique contributions

BACKUP

- ❖ Data taking by STAR at RHIC: $3 < \sqrt{s_{NN}} < 200$ GeV ($750 < \mu_B < 25$ MeV)

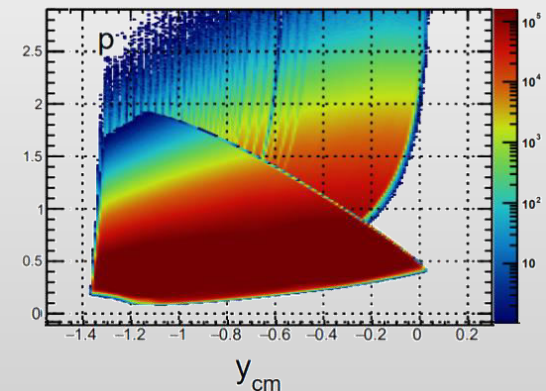
Au+Au Collisions at RHIC											
Collider Runs						Fixed-Target Runs					
	$\sqrt{s_{NN}}$ (GeV)	#Events	μ_B	y_{beam}	run		$\sqrt{s_{NN}}$ (GeV)	#Events	μ_B	y_{beam}	run
1	200	380 M	25 MeV	5.3	Run-10, 19	1	13.7 (100)	50 M	280 MeV	-2.69	Run-21
2	62.4	46 M	75 MeV		Run-10	2	11.5 (70)	50 M	320 MeV	-2.51	Run-21
3	54.4	1200 M	85 MeV		Run-17	3	9.2 (44.5)	50 M	370 MeV	-2.28	Run-21
4	39	86 M	112 MeV		Run-10	4	7.7 (31.2)	260 M	420 MeV	-2.1	Run-18, 19, 20
5	27	585 M	156 MeV	3.36	Run-11, 18	5	7.2 (26.5)	470 M	440 MeV	-2.02	Run-18, 20
6	19.6	595 M	206 MeV	3.1	Run-11, 19	6	6.2 (19.5)	120 M	490 MeV	1.87	Run-20
7	17.3	256 M	230 MeV		Run-21	7	5.2 (13.5)	100 M	540 MeV	-1.68	Run-20
8	14.6	340 M	262 MeV		Run-14, 19	8	4.5 (9.8)	110 M	590 MeV	-1.52	Run-20
9	11.5	157 M	316 MeV		Run-10, 20	9	3.9 (7.3)	120 M	633 MeV	-1.37	Run-20
10	9.2	160 M	372 MeV		Run-10, 20	10	3.5 (5.75)	120 M	670 MeV	-1.2	Run-20
11	7.7	104 M	420 MeV		Run-21	11	3.2 (4.59)	200 M	699 MeV	-1.13	Run-19
						12	3.0 (3.85)	2000 M	750 MeV	-1.05	Run-18, 21

- ❖ A very impressive and successful program with many collected datasets, already available and expected results

- ❖ Limitations:

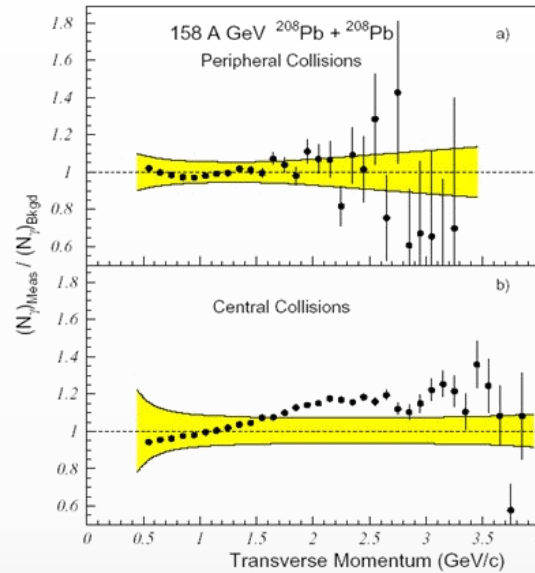
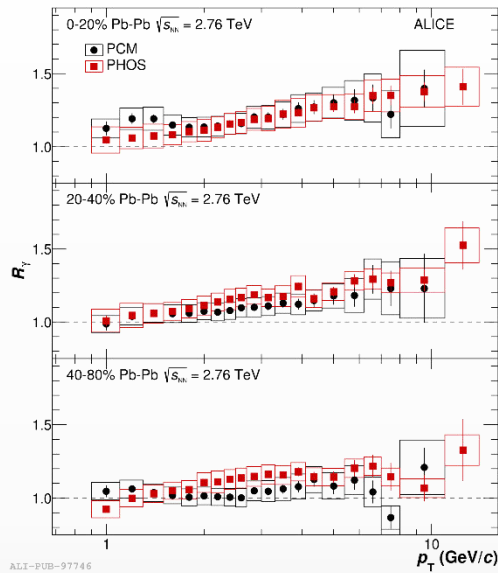
- ✓ Au+Au collisions only
- ✓ Among the fixed-target runs, only the 3 GeV data have full mid-rapidity coverage for protons ($|y| < 0.5$), which is crucial for physics observables

Au+Au @ 3.9 GeV

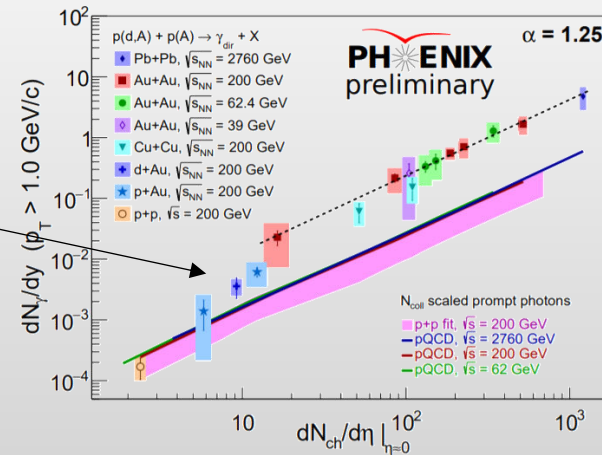
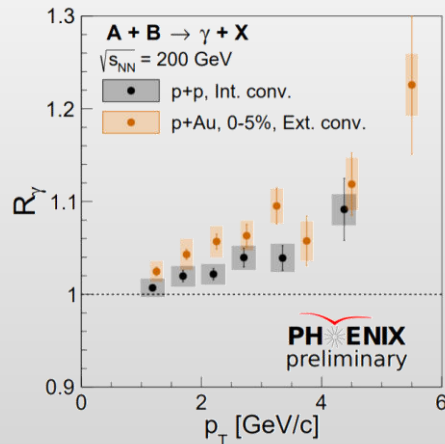


Comparison to higher energies

- $R_\gamma \sim 1.05-1.2$ in heavy-ion collisions at SPS/RHIC/LHC, $\sqrt{s_{NN}} = 17.2-2760$ GeV



- $R_\gamma \sim 1.05$ is on the verge of experimental measurability (PHENIX in pp/pA@200, $\geq 2\sigma$)

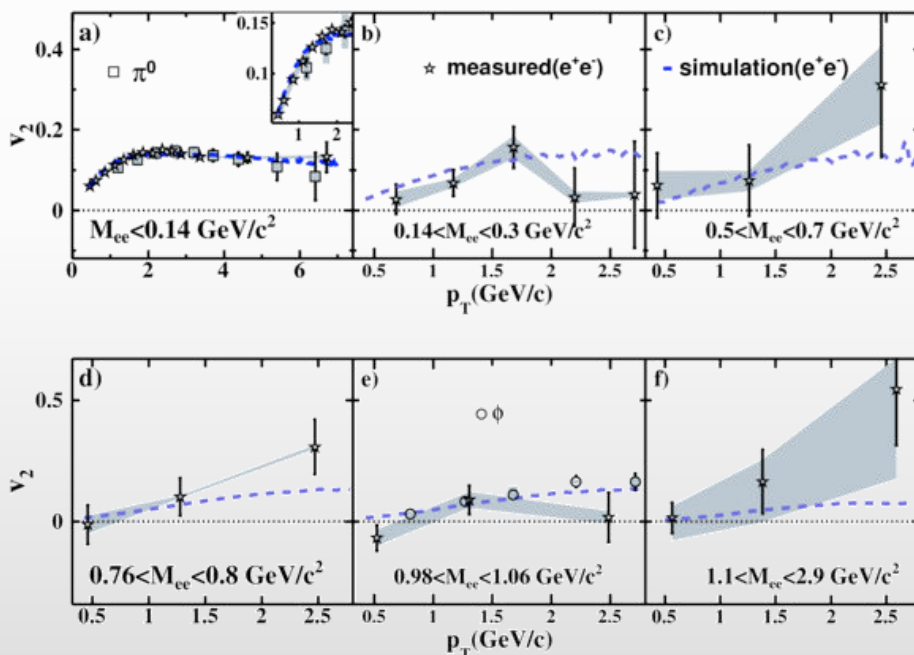


Prospects (II)

□ v_2 of thermal radiation

- Very challenging measurement
- v_2 as a function of p_T in different invariant mass regions probes the properties of the medium at different stages, from QGP to hadron-gas, provide an independent confirmation about the origin of the thermal radiation

Inclusive dielectron v_2
STAR PRC 90, 64904 (2014)

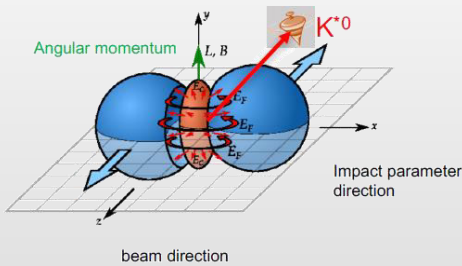
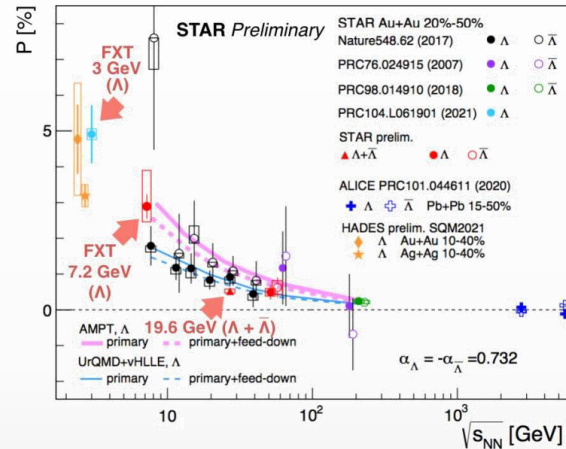
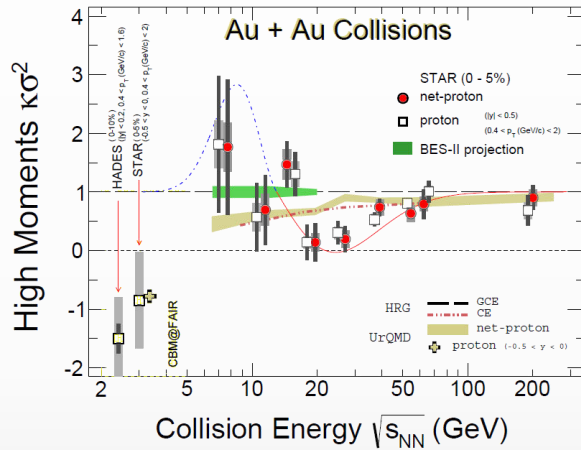


PHENIX, PRC 93, 014904 (2016)

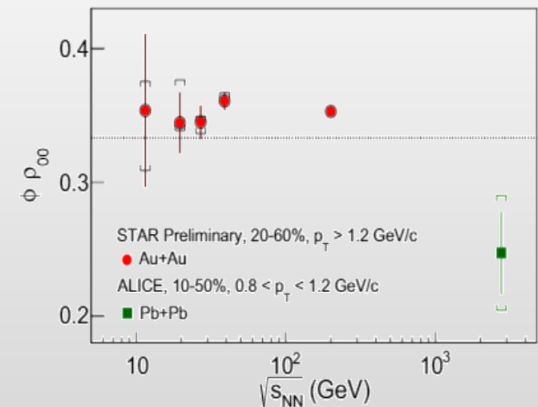
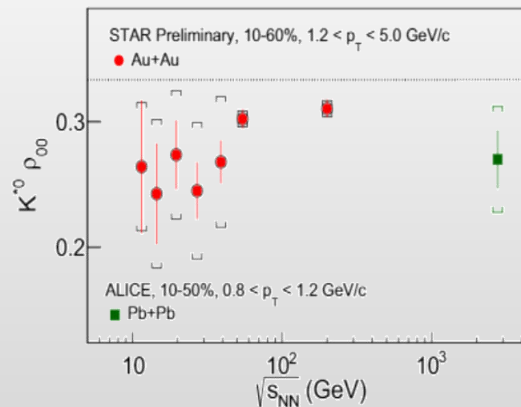
Challenge: isolate the v_2 of the excess dileptons

NICA → extensive program of dielectron measurements at $\sqrt{s_{NN}} = 2-11$ GeV

- ❖ Critical fluctuations for (net)proton/kaon multiplicity distributions
- ❖ Global hyperon polarization in mid-central A+A collisions (Λ , Ξ , Ω and antiparticles)
- ❖ Spin alignment of vector mesons ($K^*(892)$, $\phi(1020)$)



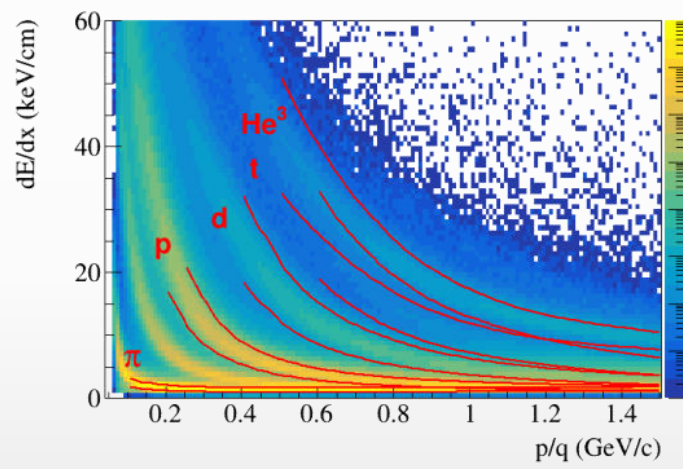
$$\frac{dN}{d\cos\theta} = N_0 [1 - \rho_{0,0} + \cos^2\theta (3\rho_{0,0} - 1)]$$



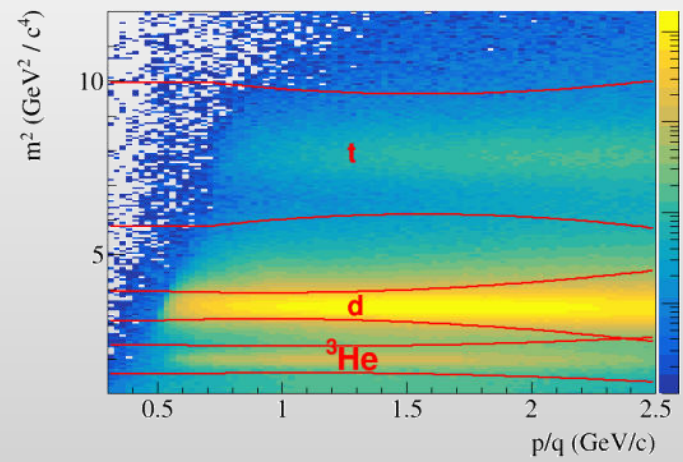
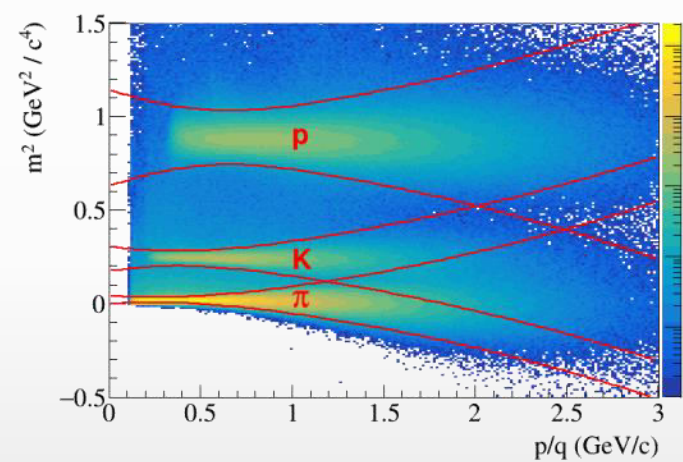
Task for the MPD: extra points in the energy range 4-11 GeV with small uncertainties

- ❖ NICA can deliver different ion beam species and energies:
 - ✓ Targets of interest (C = astronaut, Si = electronics, Al = spacecraft) + He, C, O, Si, Fe, etc.
- ❖ No data exist for projectile energies > 3 GeV/n

dE/dx vs momentum in TPC



m^2 vs. momentum in TOF



MPD has excellent light fragment identification capabilities in a wide rapidity range → unique capability of the MPD in the NICA energy range